

1 **Substrate preferences of long-chain acyl-CoA synthetase and diacylglycerol acyltransferase**
2 **contribute to enrichment of flax seed oil with α -linolenic acid**

3 Yang Xu¹, Roman Holic^{2,3,4}, Darren Li¹, Xue Pan¹, Elzbieta Mietkiewska¹, Guanqun Chen¹, Jocelyn
4 Ozga¹, and Randall J. Weselake^{1*}

5 ¹Department of Agricultural, Food and Nutritional Science, University of Alberta, Edmonton,
6 Alberta, Canada T6G 2P5

7 ²Institute of Animal Biochemistry and Genetics, Centre of Biosciences, Slovak Academy of
8 Sciences, Dubravska cesta 9, Bratislava, Slovakia

9 ³Biomedical Center Martin, Jessenius Faculty of Medicine in Martin, Comenius University in
10 Bratislava, Bratislava, Slovakia

11 ⁴Department of Pathophysiology, Jessenius Faculty of Medicine in Martin, Comenius University in
12 Bratislava, Bratislava, Slovakia

13

14 * To whom correspondence should be addressed: Randall J. Weselake, Department of Agricultural,
15 Food and Nutritional Science, University of Alberta, Edmonton, Alberta, Canada T6G 2P5, Phone:
16 (+1) 306 261-0560; E-mail: randall.weselake@ualberta.ca

17

18 **Running title:** Flax LACS and DGAT prefer α -linolenic acid

19

20 **Highlights:**

21 Flax long-chain acyl-CoA synthetase (LACS) 8 shows substrate preference towards α -linolenic acid.

22 Flax diacylglycerol acyltransferase (DGAT) 2 has strong preference towards linolenoyl-CoA.

23 LACS8 and DGAT2 may cooperate and contribute to the biosynthesis of α -linolenic acid-enriched
24 triacylglycerol.

25 **Abstract:**

26 Seed oil from flax (*Linum usitatissimum*) is enriched in α -linolenic acid (ALA; 18:3 $\Delta^{9cis,12cis,15cis}$) but
27 the biochemical processes underlying the enrichment of flax seed oil with this polyunsaturated fatty
28 acid are not fully elucidated. Here, a potential process involving the catalytic actions of long-chain
29 acyl-CoA synthetase (LACS) and diacylglycerol acyltransferase (DGAT) is proposed for ALA
30 enrichment in triacylglycerol (TAG). LACS catalyzes the ATP-dependent activation of free fatty
31 acid to form acyl-CoA, which in turn may serve as an acyl-donor in the DGAT-catalyzed reaction
32 leading to TAG. To test this hypothesis, flax *LACS* and *DGAT* cDNAs were functionally expressed
33 in *Saccharomyces cerevisiae* strains to probe their possible involvement in the enrichment of TAG
34 with ALA. Among the identified flax LACSs, LuLACS8A exhibited significantly enhanced
35 specificity for ALA over oleic acid (18:1 Δ^{9cis}) or linoleic acid (18:2 $\Delta^{9cis,12cis}$). Enhanced α -
36 linolenoyl-CoA specificity was also observed in the enzymatic assay of flax DGAT2 (LuDGAT2-3),
37 which displayed ~20 times increased preference towards α -linolenoyl-CoA over oleoyl-CoA.
38 Moreover, when *LuLACS8A* and *LuDGAT2-3* were co-expressed in yeast, both *in vitro* and *in vivo*
39 experiments indicated that the ALA-containing TAG enrichment process was operative between
40 LuLACS8A and LuDGAT2-3-catalyzed reactions. Overall, the results support the hypothesis that
41 the cooperation between the reactions catalyzed by LACS8 and DGAT2 may represent a route to
42 enrich ALA production in the flax seed oil.

43

44 **Key words:** LACS; DGAT; seed oil biosynthesis; polyunsaturated fatty acids; *Linum usitatissimum*;
45 *Saccharomyces cerevisiae*

46

47 **Abbreviations list:**

48 The abbreviations used are: ALA, α -linolenic acid; DAG, *sn*-1,2-diacylglycerol; DGAT,
49 diacylglycerol acyltransferase; ER, endoplasmic reticulum; FAME, fatty acid methyl ester; GC, gas
50 chromatography; LA, linoleic acid; LACS, long-chain acyl-CoA synthetase; LPCAT,
51 lysophosphatidylcholine acyltransferase; OA, oleic acid; PC, phosphatidylcholine; PDAT,
52 phospholipid:diacylglycerol acyltransferase; PDCT, phosphatidylcholine:diacylglycerol
53 cholinephosphotransferase; PUFA, polyunsaturated fatty acid; QM, quadruple mutant; TAG,
54 triacylglycerol; TLC, thin layer chromatography.

55 Introduction

56 The seed oil of *Linum usitatissimum* (flax, linseed) is enriched in α -linolenic acid (ALA;
57 $18:3\Delta^{9cis,12cis,15cis}$) and of value in nutraceutical and industrial applications [1]. In developing seeds of
58 oleaginous plant species, monounsaturated fatty acids are produced in the plastids. Polyunsaturated
59 fatty acids (PUFAs) such as ALA, however, are synthesized on membrane lipid (e.g.
60 phosphatidylcholine [PC]), and then transferred into triacylglycerol (TAG) in processes involving
61 acyl-editing [2,3]. Acyl-editing is crucial for PUFA-enrichment processes, and is considered a
62 cooperative metabolic network of a number of enzymes [4]. Recent research has demonstrated that
63 developing flax seed has indeed evolved various mechanisms for effectively incorporating ALA
64 into seed TAG. These mechanisms include acyltransferase action [1,5] and removal of the
65 phosphocholine headgroup of ALA-enriched PC so as to produce ALA-enriched *sn*-1,2-
66 diacylglycerol (DAG) for the Kennedy pathway leading to TAG [6].

67 Long-chain acyl-CoA synthetase (LACS, EC 6.2.1.3) may also play a role in transferring
68 ALA into flax seed TAG. Indeed, LACS provides an important function in TAG biosynthesis and
69 other lipid metabolic pathways in plants, catalyzing the ATP-dependent activation of free fatty acids
70 to form acyl-CoAs. In *Arabidopsis thaliana* (hereafter, *Arabidopsis*), nine *LACS* genes have been
71 found to participate in fatty acid and glycerolipid metabolism [7]. While AtLACS6 and AtLACS7
72 have been found to be involved in the activation of fatty acids for β -oxidation during seedling
73 development [8,9], AtLACS1, AtLACS2 and AtLACS4 appear to function in surface lipid
74 biosynthesis [10–14]. In addition to the essential functions in plant development, LACS is also
75 involved in TAG biosynthesis. *De novo* synthesized free fatty acids exported from the plastid are
76 activated to acyl-CoAs by LACS action on the outside of the plastid thus providing cytosolic acyl-
77 CoAs for use in TAG assembly in the endoplasmic reticulum (ER) [4]. In addition, the activation of
78 modified fatty acids released from PC by phospholipase A₂ also requires LACS action [15,16].

79 The identification of specific LACS involved in plant TAG biosynthesis, however, has
80 remained elusive. The plastidial outer envelope-associated AtLACS9 was suggested to activate
81 plastidially-derived fatty acids together with AtLACS1 [17]. A more recent study, however,
82 reported that instead of being involved in exporting fatty acids from the plastid, AtLACS9, together
83 with AtLACS4 and AtLACS8, contributed to lipid trafficking from the ER to the plastid [18]. In
84 addition to AtLACS9, ER-localized AtLACS8 has also been proposed to be involved in TAG
85 biosynthesis [19]. *AtLACS8* is highly and predominantly expressed during the oil deposition phase

86 of seed development, although disruption of *AtLACS8* itself leads to no effect on seed oil content in
87 *Arabidopsis* [17]. In the developing seeds of *Arabidopsis*, sunflower (*Helianthus annuus*), rice
88 (*Oryza sativa*), and castor (*Ricinus communis*) and a diatom (*Thalassiosira pseudonana*),
89 specialized LACSs with distinct substrate specificities have been identified, suggesting their
90 possible role in transferring different fatty acids [7,20–23]. There are, however, no reports on the
91 role of LACS in ALA enrichment in flax.

92 Acyl-CoAs resulting from LACS action provide the acyl chains for TAG and the reactions
93 involve the sequential acylation of *sn*-glycerol-3-phosphate via the catalytic actions of three
94 different acyl-CoA-dependent acyltransferases [24,25]. Diacylglycerol acyltransferase (DGAT, EC
95 2.3.1.20) catalyzes the final acyl-CoA-dependent acylation of DAG and acyl-CoA to form TAG. In
96 some oleaginous plant species, the level of DGAT activity has a substantial effect on the flow of
97 carbon into seed TAG, and thus may represent a bottleneck in TAG formation [26]. At least two
98 forms of membrane-bound DGAT with very different amino acid sequences have been designated
99 DGAT1 and DGAT2. DGAT1 appears to contribute more generally to TAG biosynthesis, whereas
100 DGAT2, by displaying unique substrate specificity, seems to be more important in the formation of
101 TAG containing unusual fatty acids such as ricinoleic acid (12-OH 18:1 Δ^{9cis}) and α -eleostearic acid
102 (18:3 $\Delta^{9cis,11trans,13trans}$) from castor and tung tree (*Vernicia fordii*), respectively [27–29]. Recently,
103 DGAT1 has also been linked to the accumulation of fatty acyl chains <16 carbon in seed TAGs in
104 plants such as palm (*Elaeis guineensis*) [30] and *Cuphea* [31]. Previous characterization of flax
105 DGAT1 has shown that DGAT1 indeed displayed a slight preference towards α -linolenoyl-CoA *in*
106 *vitro* [32], but the substrate specificity of flax DGAT2 remain uncharacterized.

107 Since evolved forms of LACSs and DGATs selective for unusual fatty acid exist naturally,
108 it is possible that flax contains ALA-selective LACSs and DGATs contributing to transferring ALA
109 from PC into TAG. In this study, the putative *LACS* genes involved in TAG biosynthesis in flax
110 were identified, and the effects of the encoded LACS enzymes and flax DGAT2 on ALA
111 enrichment in TAG were evaluated. Several cDNAs encoding putative LACS enzymes were first
112 isolated from flax, and among the encoded enzymes, LuLACS8A displayed an increased substrate
113 preference towards ALA. Furthermore, LuDGAT2 exhibited enhanced preference towards α -
114 linolenoyl-CoA. To test whether the α -linolenoyl-CoA from ALA-selective LuLACS8A action
115 could be incorporated into TAG by LuDGAT2 action, *LuLACS8A* and *LuDGAT2* were co-
116 expressed in *Saccharomyces cerevisiae* mutant *BYQMfaa1,4 Δ* (lacking TAG synthesizing ability
117 and two major LACSs, FAA1p and FAA4p) and their combined performance for enriching TAG in

118 ALA was evaluated using *in vitro* and *in vivo* assays. The results suggest that the LuLACS8A-
119 catalyzed reaction may contribute to the enhanced accumulation of ALA in flax oil by cooperation
120 with the LuDGAT2-catalyzed reaction.

121

122 **Experimental**

123 **Identification of *LuLACS* genes and sequence analysis**

124 AtLACS8 and 9 protein sequences were used to query the flax genomic database (v1.0;
125 www.phytozome.net/flax). Sequence alignments of LACS proteins were conducted using ClustalW
126 in MEGA 7 under the default settings [33]. A neighbour-joining tree was built using the same
127 software under the *Poisson* model, pairwise deletion and 1000 bootstrap repetitions. For calculating
128 the *Ks* values (synonymous substitution rates) for each gene pair, the aligned protein sequences
129 were used to guide the alignment of their corresponding coding sequences using PAL2NAL server
130 (<http://www.bork.embl.de/pal2nal/>). *Ks* values were calculated by codon-based likelihood method
131 with the F3X4 codon frequency model in CodeML program of the PAML version 4 software [34].
132 The approximate divergence time (T) was calculated using the mean *Ks* value by following
133 equation $T = Ks/2\lambda$, where λ is the synonymous substitution rate of 6.1×10^{-9} substitutions per
134 synonymous site per year [35]. The theoretical molecular mass and isoelectric point value of the
135 deduced LuLACS proteins were calculated by Compute pI/Mw server
136 (http://web.expasy.org/compute_pi/). The topology organization of LACSs was predicted using the
137 following algorithms: TMpred [36], TMHMM [37], SOSUI [38], and Phobius [39]. A membrane
138 protein topology prediction of LuLACS8A was visualized by Protter [40].

139 **Isolation of *LuLACS* cDNAs and plasmid construction**

140 Six putative *LACS* genes were identified and the primer pairs (Table S1) were designed
141 accordingly for cDNA amplification. Specific restriction sites were introduced in forward (Not I)
142 and reverse primers (Sal I). A Kozak translation initiation sequence (*italic*) was also introduced in
143 the forward primer of *LuLACS8A* to improve the translation of the protein. In order to amplify the
144 target genes, total mRNA was extracted from developing flax embryos (12 days after flowering)
145 using RNeasy plant mini kit (Qiagen, Toronto, ON, Canada) and then cDNAs were synthesized
146 using SuperScript III reverse transcriptase (Invitrogen, Burlington, ON, Canada). The target genes
147 were amplified by PCR reaction using the resulting cDNA as the template and the generated PCR
148 products were subcloned between the corresponding restriction sites of the pYES2 vector. pYES2

149 vector is a modified pYES2.1 vector (pYES2.1-V5/HIS vector, Invitrogen) which was constructed
150 in our laboratory.

151 The *LuDGAT1-1* cDNA was cloned into the multiple cloning site 2 (MCS2) of the pESC-
152 URA vector in the previous study [1]. Codon sequence of *LuDGAT2-3* was optimized for
153 expression in *S. cerevisiae* by Eurofins Genomics (Toronto, ON, Canada) and was then subcloned
154 into the MCS2 of the pESC-URA vector. The coding sequences of *LuDGAT1-1*, *LuDGAT2-3* and
155 codon-optimized *LuDGAT2-3* were cloned into the pYES-NT vector (Invitrogen), under the control
156 of the *GAL1* promoter and with the addition of an N-terminal His-tag.

157 The co-expression constructs were prepared as described previously [32]. Briefly, the
158 region from *CYC1* terminator to *ADHI* terminator of pESC construct (pESC-URA, *LuDGAT1-1* in
159 pESC, or codon-optimized *LuDGAT2-3* in pESC) and the entire plasmid of pYES2 or *LuLACS8A* in
160 pYES2 were amplified by PCR and the resulting DNA fragments were assembled using the method
161 described by Gibson [41]. Six different plasmids from the DNA fragments assembly are referred to
162 as: 1) *pLACS8A+DGAT1-1* contains both *LuLACS8A* and *LuDGAT1-1* genes; 2)
163 *pLACS8A+DGAT2-3** contains both *LuLACS8A* and codon-optimized *LuDGAT2-3* genes; 3)
164 *pLACS8A* contains only *LuLACS8A*; 4) *pDGAT1-1* contains only *LuDGAT1-1*; 5) *pDGAT2-3**
165 contains only codon-optimized *LuDGAT2-3*; 6) pNC is the control plasmid. The expression of all
166 above genes in the co-expression constructs are under the *GAL1* promoter. All the plasmids used in
167 the current study are listed in Table S2. The integrity of all constructs was confirmed by DNA
168 sequencing.

169 **Yeast mutant construction and heterologous expression of *LuLACS*s**

170 All the *S. cerevisiae* strains used in the current study are listed in Table S3. Wild type *S.*
171 *cerevisiae* strain BY4742 (*MAT α* , *his3 Δ 1*, *leu2 Δ 0*, *lys2 Δ 0*, *ura3 Δ 0*) was obtained from the Euroscarf
172 collection. Quadruple mutant (QM) lacking lipid droplets in BY4742 genetic background
173 (*MAT α* , *his3 Δ 1*, *leu2 Δ 0*, *lys2 Δ 0*, *ura3 Δ 0*, *are1::KanMX*, *are2::KanMX*, *dgal::KanMX*, *lro1::KanM*
174 *X*) was kindly provided by K. Athenstaedt (Graz University of Technology, Austria). Construction
175 of *BYQMfaa1,4 Δ* (*MAT α* , *his3 Δ 1*, *leu2 Δ 0*, *lys2 Δ 0*, *ura3 Δ 0*, *dgal Δ ::kanMX*, *lro1 Δ ::kanMX*, *are1*
176 *Δ ::kanMX*, *are2 Δ ::kanMX*, *faa1 Δ ::HIS3*, *faa4 Δ ::LYS2*) was described in [42]. Construction of
177 *BYfaa1,4 Δ* (*MAT α* , *his3 Δ 1*, *leu2 Δ 0*, *lys2 Δ 0*, *ura3 Δ 0*, *faa1 Δ ::HIS3*, *faa4 Δ ::LYS2*) was done in our
178 laboratory by the same approach as the *BYQMfaa1,4 Δ* [42].

179 All yeast transformation was performed using the *S.c.* EasyComp Transformation Kit
180 (Invitrogen). Transformants were selected on minimal medium plates lacking uracil (0.67% (w/v)
181 yeast nitrogen base, 0.2 % (w/v) synthetic complete medium lacking uracil (SC-Ura), 2% (w/v)
182 dextrose, and 2% (w/v) agar). For yeast culture conditions, the recombinant yeast cells were first
183 grown in liquid minimal medium (0.67% (w/v) yeast nitrogen base and 0.2 % (w/v) SC-Ura) with 2%
184 (w/v) raffinose. After overnight culture, the yeast cells were used to inoculate minimal medium
185 containing 2% (w/v) galactose and 1% (w/v) raffinose (referred as induction medium) at a starting
186 OD₆₀₀ value of 0.4. For the feeding experiment, recombinant yeasts were induced in induction
187 medium with supplementation of 200 μM various fatty acids, including oleic acid (OA, 18:1Δ^{9cis}),
188 linoleic acid (LA, 18:2Δ^{9cis,12cis}) or ALA. Fatty acids were dissolved in 0.5 M ethanol first and then
189 mixed with induction medium containing 0.1% (v/v) tyloxapol. Cultures for all experiments were
190 grown at 30°C with shaking at 220 rpm.

191 For heterologous expression of *LACS* cDNAs, the recombinant *LuLACS* plasmids were
192 transformed into *S.cerevisiae* strain *BYfaa1,4Δ*. For yeast complementation, after grown in
193 induction medium for 12 h, the recombinant yeast cells were harvested and washed with minimal
194 medium with 2% (w/v) raffinose. The cells were then centrifuged and resuspended with the same
195 medium at an OD₆₀₀ value of 0.4. Aliquots of each culture were diluted serially and 2 μL of each
196 diluted culture was spotted on induction plate containing only 100 mM OA or 45 mM cerulenin or
197 both. To disperse the fatty acids into the medium better, 1% (v/v) tyloxapol was also added into all
198 induction plates. The plates were covered by foil and incubated at dark at 30°C for 3~4 days. For
199 heterologous expression of *DGAT* cDNAs, the recombinant *LuDGAT* plasmids were transformed
200 into *S. cerevisiae* strain H1246 (*MATα are1-Δ::HIS3, are2-Δ::LEU2, dga1-Δ::KanMX4, lro1-*
201 *Δ::TRP1 ADE2*), which was kindly provided by Dr. Sten Stymne of the Swedish University of
202 Agricultural Science. For the co-expression study, the co-expression constructs were transformed
203 into *S. cerevisiae* strain *BYQMfaa1,4Δ*.

204 Nile red fluorescence assay

205 The Nile red fluorescence assay was performed as described previously [1] using a Synergy
206 H4 Hybrid reader (Biotek, Winooskit, VT, USA). In brief, 100 μL of yeast culture was placed in
207 96-well dark plate and then 5 μL of Nile red solution (0.1 mg/mL in methanol) were added. The
208 fluorescence was measured before and after the addition of Nile red solution with excitation at 485
209 nm and emission at 538 nm. The Nile red results were calculated based on the change in
210 fluorescence divided by OD₆₀₀ (ΔF/OD₆₀₀).

211 **Yeast lipid extraction and analysis**

212 Yeast lipid was extracted from approximately 30 mg of lyophilized yeast cells. For
213 quantification, 100 μ g of triheptadecanoin (C17:0 TAG) were added to each sample as a TAG
214 internal standard. The total yeast lipid were extracted using the method described previously [1].
215 The extracted lipids were separated on thin layer chromatography (TLC) plate (0.25 mm Silica gel,
216 DC-Fertigplatten, Macherey-Nagel, Germany) using hexane/diethyl ether/acetic acid (80:20:1, v/v/v)
217 as the development solvent. After visualization by primuline staining, corresponding TAG bands
218 were scraped and transmethylated by 1 mL methanolic HCl for 1 h at 80°C. The resulting fatty acid
219 methyl esters (FAMES) were extracted twice with hexane and then dried under nitrogen gas.
220 Isolated FAMES were resuspended with iso-octane before being analyzed by gas chromatography
221 (GC)/mass spectrometry (MS). The samples were separated on a capillary column DB 23 (30
222 m \times 0.25 mm \times 0.25 μ m, Agilent Technologies, Wilmington, DE, USA) by an Agilent 6890N GC
223 equipped with a 5975 inert XL Mass Selective Detector (Agilent Technologies) as described
224 previously [1].

225 **Protein extraction and western blotting**

226 Microsomal and cytosolic fractions were isolated from yeast cells as described previously
227 [1]. Briefly, after overnight induction, the recombinant yeast cells were collected, washed and then
228 resuspended in 1 mL of lysis buffer (20 mM Tris-HCl pH 7.9, 10 mM MgCl₂, 1 mM EDTA, 5%
229 (v/v) glycerol, 300 mM ammonium sulfate and 2 mM dithiothreitol). The cells were then
230 homogenized in the presence of 0.5 mm glass beads by a bead beater (Biospec, Bartlesville, OK,
231 USA). The crude homogenate was centrifuged for 30 min at 10 000 g. To separate microsomal and
232 cytosolic fractions, the supernatant was further centrifuged at 105 000 g for 70 min. The
233 microsomal pellet was resuspended in 3 mM imidazole buffer (pH 7.4) containing 125 mM sucrose.
234 All procedures were conducted at 4°C. Microsomal suspensions and supernatant samples (cytosolic
235 fractions) were kept at -80°C before use. The crude protein concentration was determined using the
236 Bradford assay with BSA as a standard [43].

237 For the detection of C-terminal V5-tagged recombinant proteins, 6.5 μ g of microsomal and
238 cytosolic proteins were separated by 8-16% gradient Mini-Protean TGX Precast Gels (Bio-Rad,
239 Mississauga, ON, Canada) and then transferred to polyvinylidene difluoride membrane (Amersham,
240 GE Healthcare, Mississauga, ON, Canada). After blocking with 2% ECL prime blocking reagent
241 (Amersham), the membrane was incubated with V5-HRP-conjugated antibody (Invitrogen),

242 followed by detection using ECL Advance Western Blotting Detection Kit (Amersham) by a
243 FluorChem SP imager (Alpha Innotech Corp., San Leandro, CA, USA). For N-terminal His-tagged
244 recombinant proteins, equal volumes of microsomal suspensions were loaded on the gel and the
245 target proteins were detected using anti-HisG-HRP antibody (Invitrogen).

246 ***In vitro* enzyme assays**

247 *LACS assay*

248 LACS assay was conducted according to the procedure described by de Azevedo Souza et
249 al. [44] and Shockey et al. [7], with slight modifications. The enzyme assay was conducted at 30°C
250 with shaking for 5 min in a reaction mixture containing 100 mM Bis-Tris-propane (pH 7.6), 10 mM
251 MgCl₂, 5 mM ATP, 2.5 mM dithiothreitol, 1 mM CoA, 20 μM [1-¹⁴C] fatty acid (OA, 56.3
252 mCi/mmol; LA, 58.2 mCi/mmol; ALA, 51.7 mCi/mmol; PerkinElmer, Waltham, MA, USA) and 10
253 μg of microsomal protein in a total volume of 100 μl. The reaction was initiated by addition of
254 microsomal protein and quenched with 100 μL of 10% (v/v) acetic acid in isopropanol and
255 extracted 4 times with 900 μL of 50% (v/v) isopropanol saturated hexane. Aliquots of the aqueous
256 phase were analyzed for radioactivity by a LS 6500 multi-purpose scintillation counter (Beckman-
257 Coulter, Mississauga, ON, Canada).

258 *DGAT assay*

259 DGAT assay was performed as described previously [32]. Briefly, the enzyme assay was
260 conducted at 30°C with shaking in a 60-μL reaction mixture containing 200 mM HEPES-NaOH
261 (pH 7.4), 3.2 mM MgCl₂, 333 μM *sn*-1,2-diolein dispersed in 0.2% (v/v) Tween 20, 15 μM [1-¹⁴C]
262 oleoyl-CoA (55 μCi/μmol) (PerkinElmer), and microsomal protein. The amount of microsomal
263 protein and reaction time were as follows: for LuDGAT1-1, 2 μg of microsomal protein and a 4 min
264 reaction were adopted; for LuDGAT2-3 and codon-optimized LuDGAT2-3, 10 μg of microsomal
265 protein and a 30 min reaction were adopted. The reaction was then quenched with 10 μL of 10%
266 (w/v) SDS. The entire reaction mixture was spotted onto a TLC plate (0.25 mm Silica gel, DC-
267 Fertigplatten) and then resolved with hexane/diethyl ether/acetic acid (80:20:1, v/v/v). After
268 visualized by phosphorimaging (Typhoon Trio Variable Mode Imager, GE Healthcare),
269 corresponding TAG spots were scraped and radioactivity was quantified by a LS 6500 multi-
270 purpose scintillation counter (Beckman-Coulter). For the substrate specificity assay, radiolabelled
271 oleoyl-CoA or α-linolenoyl-CoA was synthesized from [1-¹⁴C] OA (56.3 mCi/mmol) and ALA

272 (51.7 mCi/mmol), respectively, as described by Taylor et al. [45] and 15 μ M of radiolabeled acyl-
273 CoA was used in the DGAT assay.

274 *LACS-DGAT assay*

275 The LACS-DGAT assay was performed at 30°C with shaking for 15 min or 2 h. The
276 reaction mixture contained 200 mM HEPES-NaOH (pH 7.4), 3.2 mM MgCl₂, 333 μ M *sn*-1,2-
277 diolein dispersed in 0.2% (v/v) Tween 20, 5 mM ATP, 2.5 mM dithiothreitol, 1 mM CoA, 10 μ M
278 [1-¹⁴C] linolenic acid (51.7 mCi/mmol) and 10 μ g of microsomal protein in a total volume of 60 μ L.
279 The reaction was initiated by adding microsomal protein and quenched with 10 μ L of 10% (w/v)
280 SDS. The total reaction mixture was then separated on the TLC plate and the radioactivity of the
281 corresponding TAG and acyl-CoA spots was analyzed as described above.

282 **Statistical analysis**

283 Data are shown as means \pm standard deviation (S.D.) or standard error (S.E.) for the number
284 of independent experiments indicated. Statistical analysis was performed using the SPSS statistical
285 package (SPSS 16.0, Chicago, IL, USA). Significant differences between two groups were assessed
286 using a two-tailed Student's t-test. The Levene's test was used to test equality of variance. When the
287 variances were equal, the unpaired Student's t-test assuming equal variances was performed. When
288 the variances were unequal, the unpaired Student's t-test with Welch corrections assuming unequal
289 variances was used. For multiple comparisons, one-way analysis of variance (ANOVA) with
290 Tukey's post-hoc analysis was used. In cases where the assumption of homogenous variances was
291 not met (tested by Levene's test), Welch's robust test followed by Games-Howell post hoc test was
292 performed.

293

294 **Results**

295 **Identification and characterization of *LACS* cDNAs and deduced amino acid sequences**

296 To identify putative *LACS* genes for TAG biosynthesis from flax, AtLACS8 and AtLACS9
297 protein sequences were used to query the flax genomic database (v1.0). Six putative *LACS* genes
298 were identified and the encoded LuLACS proteins were separated into two groups (AtLACS8-like
299 or AtLACS9-like group) based on phylogenetic analysis, and thus were designated as LuLACS8A,
300 8B, 9A, 9B, 9C, and 9D in this study (Fig. 1A). LuLACSs were more closely related to the LACSs
301 from castor, which also belongs to the order *Malpighiales*. The AtLACS8-like group and

302 AtLACS9-like group share 70.4% and 75.2% pairwise identity, respectively, whereas the pairwise
303 identity for all selected LACS proteins is 67.9%. One major difference in deduced LACS protein
304 sequences between the two LACS groups resides in the N-terminal region (Fig. 1B). The presence
305 of a hydrophilic N-terminal extension, which was predicted as a possible signal sequence, was
306 identified from AtLACS8-like proteins rather than AtLACS9-like proteins (Fig. 1B), probably
307 resulting in the different subcellular localizations and functions of these two groups of proteins.
308 Indeed, two AtLACS9-like proteins including AtLACS9 and *H. annuus* LACS1 (HaLACS1), have
309 been found to reside in the plastid, whereas AtLACS8 and HaLACS2 from the AtLACS8-like
310 proteins group have been shown to localize in the ER [17,18,21,46]. The most conserved region in
311 the N-termini of proteins from both LACS groups contains a potential membrane-spanning segment
312 (Table S4 and Fig. S1), which is similar to the common architecture of very-long-chain acyl-CoA
313 synthetase [47,48]. To further characterize the *LACS* genes in flax, a polyploidy crop, the genes and
314 their encoded proteins were further analyzed in detail. The overviews of corresponding cDNAs and
315 the encoded proteins of *LuLACSs* are presented in Table S5. Although the sequence similarity of all
316 these encoded proteins is 59.2%, the protein sequences representing each cDNA pair share very
317 high identity (Table S6), with similarity from 96% (LuLACS8A and 8B) to 98% (LuLACS 9A and
318 9B; LuLACS 9C and 9D). Analysis of the synonymous substitution rates (*K_s*, Table S6) observed
319 within cDNA pairs indicated that divergence occurred approximately 6.8 million years ago, which
320 is consistent with the recent genome duplication event (5-9 million years ago) in flax [49].

321 **Heterologous expression of *LuLACSs* in *S. cerevisiae* *BYfaa1,4A***

322 Considering the high similarity between *LuLACS8A* and *8B*, *9A* and *9B*, and *9C* and *9D*,
323 respectively (Fig. 1A and Table S6), only *LuLACS8A*, *9A* and *9C* were expressed in *S. cerevisiae*
324 mutant *BYfaa1, 4A* to verify their function. The yeast mutant *BYfaa1, 4A* has both *FAA1* and *FAA4*
325 genes knocked out which together encode LACS enzymes accounting for over 90% of LACS
326 activity in yeast [50], and thus cannot grow on media containing fatty acids and cerulenin (an
327 endogenous fatty acid synthesis inhibitor) due to defective formation of acyl-CoAs. The growth of
328 cells can be rescued by transforming with an *LACS* cDNA encoding active LACS. As shown in Fig.
329 S2, all three putative *LuLACS* cDNAs complemented the yeast mutant phenotype, indicating that
330 the *LuLACSs* encoded active LACS enzymes. Previously, plant LACSs have been shown to
331 stimulate lipid accumulation and facilitate fatty acid uptake in yeast [50–52]. To investigate whether
332 *LuLACSs* could contribute to these aspects, the yeasts producing *LuLACSs* were cultured in the
333 absence or presence of OA, LA or ALA. Neutral lipid content in yeast producing *LuLACSs*

334 cultured in the absence of exogenous fatty acids accumulated to slightly higher levels than the
335 control groups (Fig. S3A). When fatty acids were provided exogenously, yeast cultures producing
336 recombinant LuLACSs accumulated similar or higher level of total lipid (data not shown) and led to
337 an increased amount of the corresponding fatty acids in TAG compared to the control groups (Fig.
338 S3B). Together, these results indicated that LuLACSs might play roles in activating OA, LA and
339 ALA and subsequently participating in transferring these fatty acids into TAG.

340 **LuLACS8A has increased substrate specificity towards α -linolenic acid**

341 Since the fatty acid feeding results revealed that LuLACSs could utilize OA, LA or ALA as
342 substrates, we further conducted *in vitro* enzyme assays to investigate whether LuLACSs have
343 preference towards certain substrates. The microsomal and cytosolic fractions of yeast mutant
344 *BYfaa1,4 Δ* producing LuLACSs were isolated for analysis of enzyme polypeptide accumulation by
345 Western blotting. The recombinant LuLACSs were mainly localized in the microsomal fraction
346 rather than the cytosolic fraction (Fig. 2A), which was consistent with a protein topology prediction
347 of LuLACSs containing one transmembrane domain at the N-terminus (Table S4 and Fig. S1). The
348 substrate specificity of each LuLACS was then assessed by using the corresponding microsomal
349 fractions; all three LuLACSs showed activity towards OA, LA, or ALA (Fig. 2B). LuLACS8A, but
350 not 9A and 9C, displayed a substantially enhanced preference towards ALA (Fig. 2B), the dominant
351 fatty acid in flax TAG and PC [53]. Thus, LuLACS8A may be involved in the specific transferring
352 of ALA moieties released from PC of the ER to the acyl-CoA pool, which would be further utilized
353 by acyl-CoA dependent acyltransferases such as DGAT to form TAG.

354 **LuDGAT2 displays preference for substrate containing α -linolenic acid**

355 Previously, a pair of duplicated *DGAT1* genes and three *DGAT2* genes were identified in
356 flax genome by our group [1]. LuDGAT1 has been shown to display a slightly enhanced substrate
357 specificity towards α -linolenoyl-CoA [32], whereas the determination of the substrate preference of
358 LuDGAT2 was hindered due to its low activity in yeast microsomes. In order to increase its
359 polypeptide accumulation, *LuDGAT2-3* was codon-optimized for expression in yeast. The codon-
360 optimized version of *LuDGAT2-3* together with *LuDGAT1-1* or *LuDGAT2-3* were transformed into
361 *S. cerevisiae* strain H1246, which is a quadruple mutant devoid of TAG synthesis capacity [54].
362 Compared to the LacZ control, yeasts producing all three LuDGATs accumulated a similar or
363 higher amount of neutral lipid when grown in the culture with or without ALA (Fig. 3A and B). The
364 highest neutral lipid content was observed with LuDGAT1-1, whereas LuDGAT2-3 and its codon-

365 optimized version resulted in a moderate or no increase in neutral lipid content when compared to
366 the control group. Transformation of different *LuDGATs* into yeast cells also affected the fatty acid
367 composition of yeast TAG differentially. Yeasts producing LuDGAT2-3, or LuDGAT2-3 encoded
368 by the codon-optimized cDNA, generated TAG containing less saturated fatty acids (palmitic acid
369 [16:0] and stearic acid [18:0]) but more palmitoleic acid [16:1 Δ^{9cis}] than yeast producing
370 LuDGAT1-1 (Fig. 3C). When ALA was exogenously supplemented in the medium, yeast producing
371 LuDGAT2-3 generated TAG containing about 30% more ALA than yeasts producing LuDGAT1-1
372 and 50% higher ALA content was observed with TAG from yeast producing LuDGAT2-3 encoded
373 by the codon-optimized cDNA (Fig. 3D). These results suggest that LuDGAT2-3 may display
374 enhanced selectivity towards substrate containing ALA.

375 To further explore the substrate specificity of LuDGAT, the microsomal fractions
376 containing the recombinant enzymes were prepared from the cells and used to determine enzyme
377 activity. The microsomal enzyme activity of LuDGAT1-1 was much higher than that of LuDGAT2-
378 3 (Fig. 4A). LuDGAT2-3, encoded by the codon-optimized cDNA, brought about a 1.6-fold
379 increase in the microsomal DGAT activity compared to that of LuDGAT2-3, which was mainly
380 attributable to the increased polypeptide accumulation (Fig. 4B). The acyl donor substrate
381 specificities of microsomal LuDGAT1-1 and LuDGAT2-3, encoded by the codon-optimized cDNA,
382 were analyzed using oleoyl-CoA or α -linolenoyl-CoA. Consistent with our previous results [32],
383 LuDGAT1-1 showed preference towards α -linolenoyl-CoA over oleoyl-CoA (Fig. 4C). Even
384 though LuDGAT2-3 displayed very low activity towards oleoyl-CoA, the enzyme activity of
385 LuDGAT2-3 was markedly enhanced when using α -linolenoyl-CoA instead of oleoyl-CoA as
386 substrate (Fig. 4C). The ratio of substrate specificity for α -linolenoyl-CoA versus oleoyl-CoA was
387 up to 10-fold higher in LuDGAT2-3 than that in LuDGAT1-1 (Fig. 4D), confirming that
388 LuDGAT2-3 displayed enhanced preference towards α -linolenoyl-CoA.

389 **Cooperation between LuLACS8A and LuDGAT-catalyzed reactions in enriching TAG in** 390 **ALA**

391 Since LuLACS8A and LuDGATs displayed preference towards ALA containing substrates,
392 it was hypothesized that α -linolenoyl-CoA produced by LuLACS8A action could be utilized by
393 LuDGAT to form TAG. To test this hypothesis, *LuLACS8A* and *LuDGAT1-1*, or codon-optimized
394 *LuDGAT2-3*, were co-expressed in *S. cerevisiae* strain *BYQMfaa1,4 Δ* , respectively, which is devoid
395 of TAG synthesis combined with low LACS activity. Yeasts co-expressing *LuLACS8A* and

396 *LuDGAT1-1*, or *LuDGAT2-3* accumulated large amounts of neutral lipid when cultured in the
397 absence or presence of exogenous ALA, whereas expression of empty vector *pNC* or *LuLACS8A*
398 alone failed to complement neutral lipid synthesis (Fig. 5A and B). Production of *LuDGAT1-1* or
399 *LuDGAT2-3* in the yeast mutant resulted in the accumulation of neutral lipids at a lower level than
400 that from the co-expression groups (Fig. 5A and B), probably due to a limitation in the acyl-CoA
401 pool. In agreement with earlier observations (Fig. 3C and D), expression of *LuDGAT2-3* and
402 *LuLACS8A*, or each cDNA alone, in the yeast mutant generated TAG containing less saturated fatty
403 acids but more palmitoleic acid than yeasts expressing constructs containing *LuDGAT1-1* (Fig. 5C
404 and D). Co-expression of *LuLACS8A* with either *LuDGAT* resulted in TAG containing less stearic
405 acid and OA than yeast expressing *LuDGAT* alone (Fig. 5C and D), and considerable amounts of
406 ALA accumulated in yeast TAG from the co-expression group when ALA was supplied
407 exogenously (Fig. 5D). This suggested that the cooperation between *LuLACS8A* and *LuDGAT*-
408 catalyzed reactions may play a role in affecting fatty acid composition in TAG. Furthermore, co-
409 expressing *LuLACS8A* and *LuDGAT2-3* resulted in TAG containing more ALA in yeast than co-
410 expressing *LuLACS8A* and *LuDGAT1-1* (Fig. 5D), indicating that *LuDGAT2-3* may be more
411 effective in the enrichment of ALA in TAG than *LuDGAT1-1*.

412 The microsomal fractions from the recombinant yeasts transformed with different co-
413 expression vectors were isolated and used for *in vitro* enzyme assays. Incubation of ALA with yeast
414 microsomes containing *LuLACS8A* alone resulted in production of a high amount of acyl-CoA but
415 no TAG due to the absence of DGAT (Fig. 6). The production of both acyl-CoA and TAG was
416 achieved when incubating ALA with yeast microsomes containing *LuLACS8A* along with either
417 form of *LuDGAT* (Fig. 6). Consistent with the *in vivo* experiment (Fig. 5), *LuLACS8A* combined
418 with *LuDGAT2-3* was more efficient at transferring ALA into TAG than *LuLACS8A* combined
419 with *LuDGAT1-1* (Fig. 6A). Formation of TAG was also detected after incubation of ALA with
420 microsomes containing *LuDGAT1-1* or *LuDGAT2-3* alone (Fig. 6A), even though only very small
421 amounts of radiolabeled acyl-CoA were formed from the remaining LACS activity of the yeast
422 mutant background (Fig. 6B). Although the combination of *LuLACS8A* with *LuDGAT1-1* or
423 *LuDGAT2-3* formed more TAG than *LuDGAT1-1* or *LuDGAT2-3* alone after 15 min reaction,
424 extended incubation to 2 h did not result in a difference in TAG accumulation for *LuDGAT2-3* or
425 its combination with *LuLACS8A*.

426 **Discussion**

427 Seed oil from flax contains 45 to 65% ALA, which is considered one of the richest sources
428 of this essential fatty acid. Recent studies revealed that flax contains a number of lipid biosynthetic
429 enzymes displaying enhanced preference for ALA containing substrates, including DGAT1,
430 phospholipid:diacylglycerol acyltransferase (PDAT), phosphatidylcholine:diacylglycerol
431 cholinephosphotransferase (PDCT), lysophosphatidylcholine acyltransferase (LPCAT) [1,6,32].
432 Over-expression of *LuDGAT1*, *LuPDAT* or *LuPDCT* in Arabidopsis, however, resulted in no or
433 moderate increases in the ALA content of the seed oil [1,6], suggesting that other ALA-enriching
434 mechanisms are operative in flax. Therefore, we have carried out experiments using a yeast host to
435 evaluate the role of LuLACS and LuDGAT-catalyzed reactions in enriching ALA in flax seed TAG.

436 It was first suggested by Lands [15] that LACS might contribute to acyl-editing by
437 recycling fatty acid from PC back to the acyl-CoA pool. The identity of LACS involved in acyl-
438 editing and TAG biosynthesis in plants is unclear. Recently, Arabidopsis LACS4, LACS8 and
439 LACS9 were found to have overlapping functions on lipid trafficking probably via the reacylation
440 of fatty acids from PC to a specific acyl-CoA pool [18]. Indeed, in this study, LuLACS8A with
441 sequence homology to AtLACS8, was found to display increased *in vitro* substrate preference
442 towards ALA (Fig. 2), the dominant fatty acid in flax PC [53]. Consistently, the yeast fatty acid
443 feeding experiment also confirmed that LuLACS8A facilitated the activation and subsequent
444 incorporation of exogenously added ALA into yeast TAG (Fig. S3). Nonetheless, it would be
445 interesting to further explore the acyl-CoA levels in the yeast cells upon fatty acid feeding in the
446 future. This analysis may provide confirmation on the *in vivo* substrate preference of flax LACS.
447 Together, these results suggested that LuLACS8A may represent a biochemical route for
448 transferring ALA from PC into the acyl-CoA pool for use in TAG assembly. Similarly, an
449 AtLACS8 homolog (HaLACS2) in sunflower displayed substrate preference towards palmitic acid
450 and LA, which are the main fatty acids in sunflower PC [21]. In Arabidopsis, besides *AtLACS8*,
451 additional *LACS* genes, including *AtLACS1* and *AtLACS4*, were also expressed in the seed tissues
452 [17]. Therefore, AtLACS1 and AtLACS4 may have overlapping functions with AtLACS8 [18].
453 Thus, it is possible that the reacylation of PC-derived fatty acids, such as ALA, in flax involves a
454 network of overlapping LACS activities from these individual ER-localized LACS enzymes. Unlike
455 LuLACS8A, which prefers ALA, AtLACS9 homologs LuLACS9A and LuLACS9C displayed
456 broad substrate specificity towards OA, LA and ALA (Fig. 2). Similarly, AtLACS9 and its homolog
457 in sunflower have also been found to display broad substrate specificity toward C18 unsaturated

458 fatty acids [7,21]. It should be noted that due to the recent genome duplication, duplicated cDNA
459 pairs have been identified for all flax *LACS* (Table S6). One *LACS* cDNA from each pair, namely
460 *LCAS8A*, *9A* or *9C*, was further characterized. These *LACS*, however, had different protein
461 accumulation levels (Fig. 2A) and enzyme activities (Fig. 2B) in yeast, and thus complemented
462 yeast mutant growth to different extents (Fig. S2). It is possible that the other *LACS* cDNA from
463 each pair may have better expression in yeast, although the sequence similarity within each cDNA
464 pair is more than 96% (Table S6).

465 The natural presence of evolved forms of DGAT2s that are selective for PC-modified fatty
466 acids [27–29] suggested that this may also be the case for flax DGAT2. An earlier study with
467 microsomes from developing flax seed indicated that DGAT activity indeed exhibited increased
468 specificity for α -linolenoyl-CoA over oleoyl-CoA or linoleoyl-CoA [55]. The observed substrate
469 specificity was probably the net result of LuDGAT1 and LuDGAT2 action. In the current study, the
470 capabilities of recombinant LuDGATs in TAG production in yeast mutant H1246 were analyzed *in*
471 *vivo* (Fig. 3) and *in vitro* (Fig. 4). Overexpression of *LuDGAT1-1* in yeast H1246 produced a large
472 amount of TAG (Fig. 3A and B), which is consistent with its high *in vitro* enzyme activity (Fig. 4A)
473 and protein accumulation (Fig. 4B). The contribution of LuDGAT2-3 to yeast TAG accumulation
474 was less (Fig. 3A and B), probably due to its lower enzyme activity and protein accumulation (Fig.
475 4A and B). The activity of LuDGAT2-3, however, increased more than 20-fold when oleoyl-CoA
476 was replaced by α -linolenoyl-CoA (Fig. 4C and D). This was consistent with the *in vivo* ALA
477 feeding results demonstrating a 30% to 50% increase in the ALA content in TAG from yeast
478 producing LuDGAT2-3 as opposed to LuDGAT1-1 (Fig. 3). The results also relate to our previous
479 analysis of gene expression: *LuDGAT2-3* exhibited a higher expression level than *LuDGAT1-1* in
480 developing flax seed and the expression of both *LuDGAT1-1* and *LuDGAT2-3* was closely
481 correlated with ALA biosynthesis and total oil accumulation [1]. Taken together, these results
482 suggest that the LuDGAT2-3-catalyzed reaction may contribute to the enrichment of flax TAG with
483 ALA.

484 Previously, Kim et al. [56] proposed a specific acyl-CoA pool for TAG biosynthesis. Thus,
485 it is possible that flax *LACS* with unique substrate preference contributes to the transferring of ALA
486 into the specific acyl-CoA pool, which would then be utilized to form TAG by α -linolenoyl-CoA
487 selective DGAT. Indeed, the ability of the combined reactions catalyzed by LuLACS8A and
488 LuDGAT to enrich ALA in TAG was confirmed by both *in vivo* (Fig. 5) and *in vitro* (Fig. 6)
489 experiments. LuDGAT2-3 was more effective in ALA enrichment than LuDGAT1-1 (Fig. 5 and 6),

490 which is probably due to its enhanced substrate specificity for α -linolenoyl-CoA. A large amount of
491 acyl-CoA was produced when incubating ALA with yeast microsomes containing both LuLACS8A
492 and LuDGAT, but only a small amount (approximately 1-6%) of acyl-CoA was further utilized in
493 TAG formation (Fig. 6), suggesting that the DGAT-catalyzed reaction may represent a bottleneck in
494 the process of TAG formation. This is also consistent with the *in vitro* enzyme assay results for
495 LuLACS8A (Fig. 2) and either LuDGAT1-1 or LuDGAT2-3 (Fig. 4), where the microsomal
496 specific activity of LuLACS8A was approximately 20-200 times higher than that of the LuDGATs.
497 Indeed, the level of DGAT activity in developing seeds of *Brassica napus* may have a substantial
498 effect on the flow of carbon into TAG [57,58]. The possibility of limited formation of TAG,
499 because of unbalanced recombinant protein accumulation between LuLACS8A and LuDGAT in
500 yeast microsomes cannot be ruled out, even though both of the encoding cDNAs were expressed
501 under the *GALI* promoter.

502 The proposed involvement of flax DGAT2 and LACS8 in enriching TAG with ALA is
503 indeed consistent with the gene expression patterns of their encoding genes and subcellular
504 localizations. *LuDGAT2* is predominantly expressed in flax developing seeds [1]. *LuLACS8* has
505 been suggested to be expressed in embryo and seed coat rather than vegetative tissues according to
506 the expressed sequence tags (EST) data from various flax tissues [59]. In addition, the expression
507 patterns of *LuLACS8* homologs in Arabidopsis and sunflower were extensively studied [17, 21]. In
508 Arabidopsis, *AtLACS8* has been shown to be highly and predominantly expressed in the seeds
509 during the oil deposition phase of seed development [17]. Similar results have also been reported
510 for *LACS8* from sunflower [21]. Thus, *LuLACS8* may also be predominantly expressed in
511 developing flax seeds. Moreover, DGAT2 and LACS8 from a variety of species have been
512 suggested to reside in the ER [17, 21, 26, 29], providing a possible advantage in the cooperation of
513 LuLACS8- and LuDGAT2-catalyzed reactions in contributing to ALA enrichment of TAG.

514 In developing flax seed, the LuLACS8A-LuDGAT2-3 catalyzed ALA-enrichment process
515 may be coordinated with other ALA-enriching processes which include PDAT action [1], PDCT
516 action [6], and coupling of the LPCAT-catalyzed reaction to the DGAT-catalyzed reaction [32].
517 The four possible routes for ALA enrichment of TAG during flax seed development are outlined in
518 Fig. 7. In addition to the proposed ALA enrichment between LuLACS8A and LuDGAT2, ALA
519 from PC could be directly transferred into TAG via the catalytic action of LuPDAT, which has been
520 recently found to display preference towards ALA containing substrates (DAG and PC) [1].
521 Alternatively, LuPDCT has also been found to function in ALA enrichment by incorporating ALA

522 produced at the level of PC into DAG for utilization by the Kennedy pathway leading to TAG [6].
523 The resulting *sn*-1,2-DAG enriched in ALA might be an effective acyl acceptor for LuDGAT
524 (especially LuDGAT2-3) to selectively utilize α -linolenoyl-CoA or LuPDAT to form TAG.
525 Recently, Pan et al. [32] demonstrated that biochemical coupling of the LuLPCAT-catalyzed
526 reverse reaction to the LuDGAT1-catalyzed forward reaction may also serve to transfer ALA into
527 TAG. Furthermore, the enzymes involved in ALA enrichment of TAG in developing flax seed may
528 also physically interact with each other by forming enzyme complexes to assist in the ALA-
529 enrichment process. Indeed, protein-protein interaction between LPCAT and DGAT1 from
530 Arabidopsis has been shown using yeast two-hybrid assay [60]. It is also possible that other
531 additional processes contribute to enrichment of ALA in flax seed oil. For instance, the recently
532 identified glycerophosphocholine acyltransferase and lysophosphatidylcholine transacylase
533 activities from safflower microsomes represent novel reactions for PC acyl-editing [3], which may
534 also be operative in developing flax seed.

535 In conclusion, the results of this study provide further insights into the ALA-enrichment
536 process in developing flax seed. Recombinant LuLACS8A and LuDGAT2-3 were found to possess
537 enhanced preference for ALA and α -linolenoyl-CoA, respectively. *In vivo* and *in vitro* analyses of
538 ALA enrichment in TAG by the LuLACS8A-catalyzed reaction and the LuDGAT2-3-catalyzed
539 reaction indicate that this process represents a route for ALA accumulation in TAG. This process,
540 however, would be dependent on the identification of a flax phospholipase A₂ which could
541 effectively liberate ALA from PC making this PUFA available for activation by LuLACS8A. It is
542 reasonable to assume that such an α -18:3-PC-selective phospholipase A₂ exists because a candidate
543 small molecular weight phospholipase A₂ has recently been identified by Bayon et al. [16] in castor
544 for catalyzing the release of ricinoleic acid from modified PC in developing seeds from transgenic
545 Arabidopsis producing oleic acid hydroxylase.

546

547

548

549 **Acknowledgments**

550 We thank Dr. Sten Stymne from Swedish University of Agricultural Sciences for providing yeast
551 strain H1246.

552

553 **Conflict of interest**

554 The authors declare that they have no conflicts of interest with the content of this article.

555

556 **Funding information**

557 The research was supported by Alberta Innovates Bio Solutions, the Natural Sciences and
558 Engineering Research Council of Canada (RJW, RGPIN-2014-04585; GC, RGPIN-2016-05926)
559 and the Canada Research Chairs Program. We also acknowledge the support of the VEGA agency
560 grant (No. 2/0180/12) and the Research & Development Operational Programs funded by ERDF
561 (the projects TRANSMED ITMS 26240120043 and TRANSMED 2 ITMS 26240120044). YX is a
562 recipient of a scholarship from the China Scholarship Council and the Alberta Innovates Graduate
563 Student Top-up Award.

564

565 **Author contributions**

566 YX performed most of the experiments, analyzed the data and drafted the manuscript. RJW and YX
567 designed the research. RH constructed yeast mutant strains *BYfaa1,4Δ* and *BYQMfaa1,4Δ*. DL
568 helped with the isolation of *LuLACS8A* and *LuLACS9A* genes from flax. GC, RH, XP, EM, and JO
569 contributed valuable discussion during this study. All co-authors contributed to further editing the
570 manuscript.

571

572

573 **References:**

- 574 1 Pan, X., Siloto, R. M. P., Wickramarathna, A. D., Mietkiewska, E. and Weselake, R. J.
 575 (2013) Identification of a pair of phospholipid:diacylglycerol acyltransferases from
 576 developing flax (*Linum usitatissimum* L.) seed catalyzing the selective production of
 577 trilinolenin. *J. Biol. Chem.* **288**, 24173–24188.
- 578 2 Bates, P. D., Fatihi, A., Snapp, A. R., Carlsson, A. S., Browse, J. and Lu, C. (2012) Acyl
 579 editing and headgroup exchange are the major mechanisms that direct polyunsaturated fatty
 580 acid flux into triacylglycerols. *Plant Physiol.* **160**, 1530–1539.
- 581 3 Lager, I., Glab, B., Eriksson, L., Chen, G., Banas, A. and Stymne, S. (2015) Novel reactions
 582 in acyl editing of phosphatidylcholine by lysophosphatidylcholine transacylase (LPCT) and
 583 acyl-CoA:glycerophosphocholine acyltransferase (GPCAT) activities in microsomal
 584 preparations of plant tissues. *Planta* **241**, 347–358.
- 585 4 Chapman, K. D. and Ohlrogge, J. B. (2012) Compartmentation of triacylglycerol
 586 accumulation in plants. *J. Biol. Chem.* **287**, 2288–2294.
- 587 5 Pan, X., Peng, F. Y. and Weselake, R. (2015) Genome-wide analysis of
 588 *PHOSPHOLIPID:DIACYLGLYCEROL ACYLTRANSFERASE* genes in plants reveals the
 589 eudicot-wide *PDAT* gene expansion and altered selective pressures acting on the core
 590 eudicot *PDAT* paralogs. *Plant Physiol.* **167**, 887–904.
- 591 6 Wickramarathna, A. D., Siloto, R. M. P., Mietkiewska, E., Singer, S. D., Pan, X. and
 592 Weselake, R. J. (2015) Heterologous expression of flax
 593 *PHOSPHOLIPID:DIACYLGLYCEROL CHOLINEPHOSPHOTRANSFERASE (PDCT)*
 594 increases polyunsaturated fatty acid content in yeast and *Arabidopsis* seeds. *BMC*
 595 *Biotechnol.* **15**, 1–15.
- 596 7 Shockey, J. M., Fulda, M. S. and Browse, J. A. (2002) *Arabidopsis* contains nine long-chain
 597 acyl-coenzyme A synthetase genes that participate in fatty acid and glycerolipid metabolism.
 598 *Plant Physiol.* **129**, 1710–1722.
- 599 8 Fulda, M., Schnurr, J., Abbadi, A., Heinz, E. and Browse, J. (2004) Peroxisomal acyl-CoA
 600 synthetase activity is essential for seedling development in *Arabidopsis thaliana*. *Plant Cell*
 601 **16**, 394–405.
- 602 9 Fulda, M., Shockey, J., Werber, M., Wolter, F. P. and Heinz, E. (2002) Two long-chain acyl-
 603 CoA synthetases from *Arabidopsis thaliana* involved in peroxisomal fatty acid beta-
 604 oxidation. *Plant J.* **32**, 93–103.
- 605 10 Schnurr, J., Shockey, J. and Browse, J. (2004) The acyl-CoA synthetase encoded by *LACS2*
 606 is essential for normal cuticle development in *Arabidopsis*. *Plant Cell* **16**, 629–642.
- 607 11 Tang, D., Simonich, M. T. and Innes, R. W. (2007) Mutations in *LACS2*, a long-chain acyl-
 608 coenzyme A synthetase, enhance susceptibility to avirulent *Pseudomonas syringae* but
 609 confer resistance to *Botrytis cinerea* in *Arabidopsis*. *Plant Physiol.* **144**, 1093–1103.
- 610 12 Lü, S., Song, T., Kosma, D. K., Parsons, E. P., Rowland, O. and Jenks, M. A. (2009)
 611 *Arabidopsis CER8* encodes LONG-CHAIN ACYL-COA SYNTHETASE 1 (*LACS1*) that
 612 has overlapping functions with *LACS2* in plant wax and cutin synthesis. *Plant J.* **59**, 553–
 613 564.
- 614 13 Weng, H., Molina, I., Shockey, J. and Browse, J. (2010) Organ fusion and defective cuticle

- 615 function in a *lacs1 lacs2* double mutant of Arabidopsis. *Planta* **231**, 1089–1100.
- 616 14 Jessen, D., Olbrich, A., Knüfer, J., Krüger, A., Hoppert, M., Polle, A. and Fulda, M. (2011)
617 Combined activity of LACS1 and LACS4 is required for proper pollen coat formation in
618 Arabidopsis. *Plant J.* **68**, 715–726.
- 619 15 Lands, W. (1960) Metabolism of glycerolipids: II. The enzymatic acylation of lysolecithin. *J.*
620 *Biol. Chem.* **235**, 2233–2237.
- 621 16 Bayon, S., Chen, G., Weselake, R. J. and Browse, J. (2015) A small phospholipase A2- α
622 from castor catalyzes the removal of hydroxy fatty acids from phosphatidylcholine in
623 transgenic Arabidopsis seeds. *Plant Physiol.* **167**, 1259–1270.
- 624 17 Zhao, L., Katavic, V., Li, F., Haughn, G. W. and Kunst, L. (2010) Insertional mutant
625 analysis reveals that long-chain acyl-CoA synthetase 1 (LACS1), but not LACS8,
626 functionally overlaps with LACS9 in Arabidopsis seed oil biosynthesis. *Plant J.* **64**, 1048–
627 1058.
- 628 18 Jessen, D., Roth, C., Wiermer, M. and Fulda, M. (2015) Two activities of long-chain acyl-
629 CoA synthetase are involved in lipid trafficking between the endoplasmic reticulum and the
630 plastid in Arabidopsis. *Plant Physiol.* **167**, 351–366.
- 631 19 Kim, H. U., Lee, K. R., Jung, S. J., Shin, H. A., Go, Y. S., Suh, M. C. and Kim, J. B. (2015)
632 Senescence-inducible LEC2 enhances triacylglycerol accumulation in leaves without
633 negatively affecting plant growth. *Plant Biotechnol. J.* **13**, 1346–1359.
- 634 20 Tonon, T., Qing, R., Harvey, D., Li, Y., Larson, T. R. and Graham, I. A. (2005)
635 Identification of a long-chain polyunsaturated fatty acid acyl-coenzyme A synthetase from
636 the diatom *Thalassiosira pseudonana*. *Plant Physiol.* **138**, 402–408.
- 637 21 Aznar-Moreno, J. A., Venegas Calerón, M., Martínez-Force, E., Garcés, R., Mullen, R.,
638 Gidda, S. K. and Salas, J. J. (2014) Sunflower (*Helianthus annuus*) long-chain acyl-
639 coenzyme A synthetases expressed at high levels in developing seeds. *Physiol. Plant.* **150**,
640 363–373.
- 641 22 Ichihara, K., Kobayashi, N. and Saito, K. (2003) Lipid synthesis and acyl-CoA synthetase in
642 developing rice seeds. *Lipids* **38**, 881–884.
- 643 23 He, X., Chen, G. Q., Kang, S. T. and McKeon, T. A. (2007) *Ricinus communis* contains an
644 acyl-CoA synthetase that preferentially activates ricinoleate to its CoA thioester. *Lipids* **42**,
645 931–938.
- 646 24 Snyder, C. L., Yurchenko, O. P., Siloto, R. M. P., Chen, X., Liu, Q., Mietkiewska, E. and
647 Weselake, R. J. (2009) Acyltransferase action in the modification of seed oil biosynthesis. *N.*
648 *Biotechnol.* **26**, 11–16.
- 649 25 Chen, G., Woodfield, H. K., Pan, X., Harwood, J. L. and Weselake, R. J. (2015) Acyl-
650 trafficking during plant oil accumulation. *Lipids* **50**, 1057–1068.
- 651 26 Liu, Q., Siloto, R. M. P., Lehner, R., Stone, S. J. and Weselake, R. J. (2012) Acyl-
652 CoA:diacylglycerol acyltransferase: molecular biology, biochemistry and biotechnology.
653 *Prog. Lipid Res.* **51**, 350–377.
- 654 27 Burgal, J., Shockey, J., Lu, C., Dyer, J., Larson, T., Graham, I. and Browse, J. (2008)
655 Metabolic engineering of hydroxy fatty acid production in plants: RcDGAT2 drives
656 dramatic increases in ricinoleate levels in seed oil. *Plant Biotechnol. J.* **6**, 819–831.

- 657 28 Li, R., Yu, K., Hatanaka, T. and Hildebrand, D. F. (2010) *Vernonia* DGATs increase
658 accumulation of epoxy fatty acids in oil. *Plant Biotechnol. J.* **8**, 184–195.
- 659 29 Shockey, J. M., Gidda, S. K., Chapital, D. C., Kuan, J.C., Dhanoa, P. K., Bland, J. M.,
660 Rothstein, S. J., Mullen, R. T. and Dyer, J. M. (2006) Tung tree DGAT1 and DGAT2 have
661 nonredundant functions in triacylglycerol biosynthesis and are localized to different
662 subdomains of the endoplasmic reticulum. *Plant Cell* **18**, 2294–2313.
- 663 30 Aymé, L., Jolivet, P., Nicaud, J. M. and Chardot, T. (2015) Molecular characterization of the
664 *Elaeis guineensis* medium-chain fatty acid diacylglycerol acyltransferase DGAT1-1 by
665 heterologous expression in *Yarrowia lipolytica*. *PLoS One* **10**, 1–21.
- 666 31 Iskandarov, U., Silva, J. E., Kim, H. J., Andersson, M., Cahoon, R. E., Mockaitis, K. and
667 Cahoon, E. B. (2017) A specialized diacylglycerol acyltransferase contributes to the extreme
668 medium-chain fatty acid content of *Cuphea* seed oil. *Plant Physiol.* **174**, 97–109.
- 669 32 Pan, X., Chen, G., Kazachkov, M., Greer, M. S., Caldo, K. M. P., Zou, J. and Weselake, R. J.
670 (2015) *In vivo* and *in vitro* evidence for biochemical coupling of reactions catalyzed by
671 lysophosphatidylcholine acyltransferase and diacylglycerol acyltransferase. *J. Biol. Chem.*
672 **290**, 18068–18078.
- 673 33 Kumar, S., Stecher, G. and Tamura, K. (2016) MEGA7: molecular evolutionary genetics
674 analysis version 7.0 for bigger datasets. *Mol. Biol. Evol.* **33**, msw054.
- 675 34 Yang, Z. (2007) PAML 4: phylogenetic analysis by maximum likelihood. *Mol. Biol. Evol.*
676 **24**, 1586–1591.
- 677 35 Lynch, M. and Conery, J. S. (2000) The evolutionary fate and consequences of duplicate
678 genes. *Science* **290**, 1151–1155.
- 679 36 Hofmann, K. and Stoffel, W. (1993) TMbase-A database of membrane spanning protein
680 segments. *Biol. Chem. Hoppe. Seyler.* **374**, 166.
- 681 37 Krogh, A., Larsson, B., von Heijne, G. and Sonnhammer, E. (2001) Predicting
682 transmembrane protein topology with a hidden Markov model: application to complete
683 genomes. *J. Mol. Biol.* **305**, 567–580.
- 684 38 Hirokawa, T., Boon-Chieng, S. and Mitaku, S. (1998) SOSUI: classification and secondary
685 structure prediction system for membrane proteins. *Bioinformatics* **14**, 378–379.
- 686 39 Käll, L., Krogh, A. and Sonnhammer, E. L. L. (2007) Advantages of combined
687 transmembrane topology and signal peptide prediction-the Phobius web server. *Nucleic
688 Acids Res.* **35**, 429–432.
- 689 40 Omasits, U., Ahrens, C. H., Müller, S. and Wollscheid, B. (2014) Protter: interactive protein
690 feature visualization and integration with experimental proteomic data. *Bioinformatics* **30**,
691 884–886.
- 692 41 Gibson, D. G. (2011) Enzymatic assembly of overlapping DNA fragments. *Methods
693 Enzymol.* **498**, 349–361.
- 694 42 Sec, P., Garaiova, M., Gajdos, P., Certik, M., Griac, P., Hapala, I. and Holic, R. (2015)
695 Baker's yeast deficient in storage lipid synthesis uses *cis*-vaccenic acid to reduce unsaturated
696 fatty acid toxicity. *Lipids* **50**, 621–630.
- 697 43 Bradford, M. M. (1976) A rapid and sensitive method for the quantitation of microgram

- 698 quantities of protein utilizing the principle of protein-dye binding. *Anal. Biochem.* **72**, 248–
699 254.
- 700 44 de Azevedo Souza, C., Kim, S. S., Koch, S., Kienow, L., Schneider, K., McKim, S. M.,
701 Haughn, G. W., Kombrink, E. and Douglas, C. J. (2009) A novel fatty Acyl-CoA Synthetase
702 is required for pollen development and sporopollenin biosynthesis in Arabidopsis. *Plant Cell*
703 **21**, 507–525.
- 704 45 Taylor, D. C., Weber, N., Hogge, L. R. and Underhill, E. W. (1990) A simple enzymatic
705 method for the preparation of radiolabeled erucoyl-CoA and other long-chain fatty acyl-
706 CoAs and their characterization by mass spectrometry. *Anal. Biochem.* **316**, 311–316.
- 707 46 Schnurr, J. A., Shockey, J. M., Boer, G. J. De and Browse, J. A. (2002) Fatty acid export
708 from the chloroplast. Molecular characterization of a major plastidial acyl-coenzyme A
709 synthetase from Arabidopsis. *Plant Physiol.* **129**, 1700–1709.
- 710 47 Obermeyer, T., Fraisl, P., DiRusso, C. C. and Black, P. N. (2007) Topology of the yeast
711 fatty acid transport protein Fat1p: mechanistic implications for functional domains on the
712 cytosolic surface of the plasma membrane. *J. Lipid Res.* **48**, 2354–2364.
- 713 48 Lewis, S. E., Listenberger, L. L., Ory, D. S. and Schaffer, J. E. (2001) Membrane topology
714 of the murine fatty acid transport protein 1. *J. Biol. Chem.* **276**, 37042–37050.
- 715 49 Wang, Z., Hobson, N., Galindo, L., Zhu, S., Shi, D., McDill, J., Yang, L., Hawkins, S.,
716 Neutelings, G., Datla, R. and Lambert, G. (2012) The genome of flax (*Linum usitatissimum*)
717 assembled *de novo* from short shotgun sequence reads. *Plant J.* **72**, 461–473.
- 718 50 Guo, X., Jiang, M., Wan, X., Hu, C. and Gong, Y. (2014) Identification and biochemical
719 characterization of five long-chain acyl-coenzyme A synthetases from the diatom
720 *Phaeodactylum tricornutum*. *Plant Physiol. Biochem.* **74**, 33–41.
- 721 51 Tan, X., Zheng, X., Zhang, Z., Wang, Z., Xia, H., Lu, C. and Gu, S. (2014) Long chain acyl-
722 coenzyme A synthetase 4 (BnLACS4) gene from *Brassica napus* enhances the yeast lipid
723 contents. *J. Integr. Agric.* **13**, 54–62.
- 724 52 Pulsifer, I. P., Kluge, S. and Rowland, O. (2012) Arabidopsis long-chain acyl-CoA
725 synthetase 1 (LACS1), LACS2, and LACS3 facilitate fatty acid uptake in yeast. *Plant*
726 *Physiol. Biochem.* **51**, 31–39.
- 727 53 Wanasundara, P. K. J. P. D., Wanasundara, U. N. and Shahidi, F. (1999) Changes in flax
728 (*Linum usitatissimum* L.) seed lipids during germination. *J. Am. Oil Chem. Soc.* **76**, 41–48.
- 729 54 Sandager, L., Gustavsson, M. H., Stahl, U., Dahlqvist, A., Wiberg, E., Banas, A., Lenman,
730 M., Ronne, H. and Stymne, S. (2002) Storage lipid synthesis is non-essential in yeast. *J. Biol.*
731 *Chem.* **277**, 6478–6482.
- 732 55 Sørensen, B. M., Furukawa-Stoffer, T. L., Marshall, K. S., Page, E. K., Mir, Z., Forster, R. J.
733 and Weselake, R. J. (2005) Storage lipid accumulation and acyltransferase action in
734 developing flaxseed. *Lipids* **40**, 1043–1049.
- 735 56 Kim, S., Yamaoka, Y., Ono, H., Kim, H., Shim, D., Maeshima, M., Martinoia, E., Cahoon, E.
736 B., Nishida, I. and Lee, Y. (2013) AtABCA9 transporter supplies fatty acids for lipid
737 synthesis to the endoplasmic reticulum. *Proc. Natl. Acad. Sci.* **110**, 773–778.
- 738 57 Perry, H. J. and Harwood, J. L. (1993) Changes in the lipid content of developing seeds of
739 *Brassica napus*. *Phytochemistry* **32**, 1411–1415.

- 740 58 Weselake, R. J., Shah, S., Tang, M., Quant, P. A., Snyder, C. L., Furukawa-Stoffer, T. L.,
741 Zhu, W., Taylor, D. C., Zou, J., Kumar, A. and Hall, L. (2008) Metabolic control analysis is
742 helpful for informed genetic manipulation of oilseed rape (*Brassica napus*) to increase seed
743 oil content. *J. Exp. Bot.* **59**, 3543–3549.
- 744 59 Venglat, P., Xiang, D., Qiu, S., Stone, S. L., Tibiche, C., Cram, D., Alting-Mees, M., Nowak,
745 J., Cloutier, S., Deyholos, M. and Bekkaoui, F. (2011) Gene expression analysis of flax seed
746 development. *BMC Plant Biol.* **11**, 74.
- 747 60 Shockey, J., Regmi, A., Cotton, K., Neil, A., Browse, J. and Bates, P. D. (2016)
748 Identification of *Arabidopsis GPAT9* (At5g60620) as an essential gene involved in
749 triacylglycerol biosynthesis. *Plant Physiol.* **170**, 163–179.

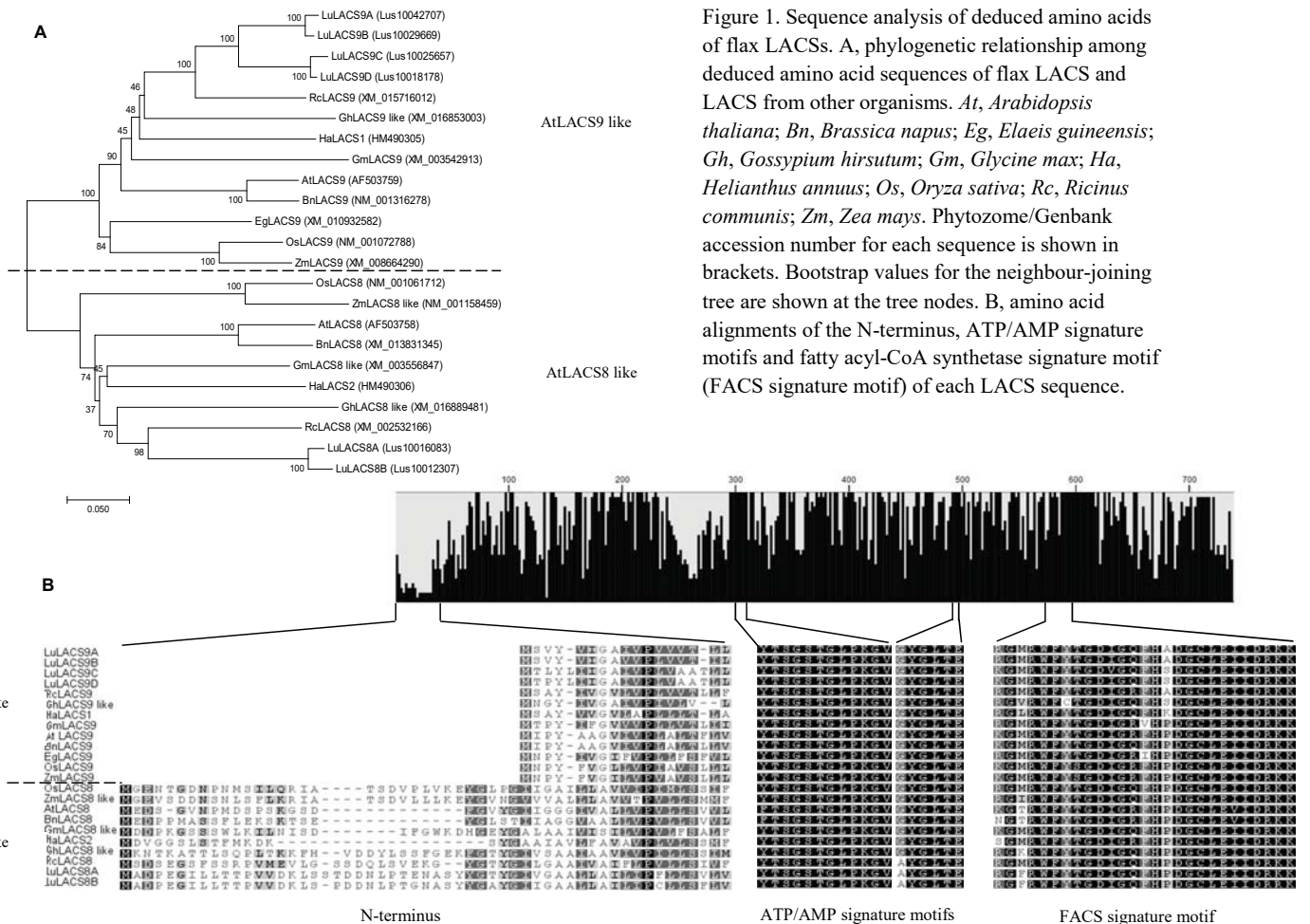


Figure 1. Sequence analysis of deduced amino acids of flax LACSs. A, phylogenetic relationship among deduced amino acid sequences of flax LACS and LACS from other organisms. *At*, *Arabidopsis thaliana*; *Bn*, *Brassica napus*; *Eg*, *Elaeis guineensis*; *Gh*, *Gossypium hirsutum*; *Gm*, *Glycine max*; *Ha*, *Helianthus annuus*; *Os*, *Oryza sativa*; *Rc*, *Ricinus communis*; *Zm*, *Zea mays*. Phytozome/Genbank accession number for each sequence is shown in brackets. Bootstrap values for the neighbour-joining tree are shown at the tree nodes. B, amino acid alignments of the N-terminus, ATP/AMP signature motifs and fatty acyl-CoA synthetase signature motif (FACS signature motif) of each LACS sequence.

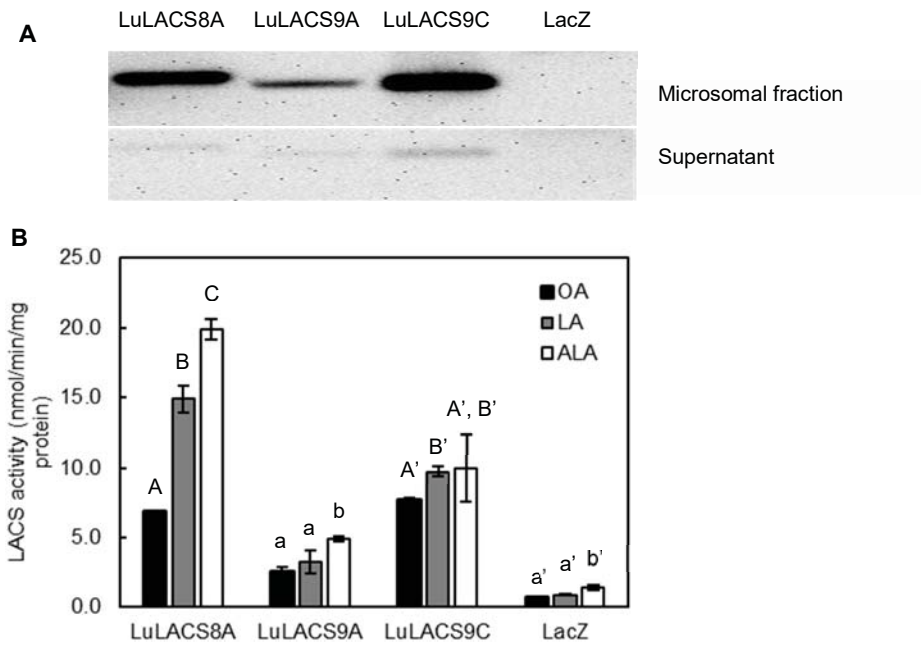


Figure 2. Localization of LuLACSs in yeast (A) and their substrate specificities (B). Microsomal preparations from the yeast mutant *BYfaa1,4Δ* producing LuLACSs were used for analysis of enzyme assay. The same amount of microsomal and cytosolic proteins was used for Western blotting analysis. Data represent means \pm S.D, n = 3-5. OA, oleic acid; LA, linoleic acid; ALA, α -linolenic acid. For B, different letters in each series (non-primed uppercase letters for LuLACS8A, non-primed lowercase letters for LuLACS9A, primed uppercase letters for LuLACS9C, and primed lowercase letters for LacZ control) indicate significant differences in the substrate specificity of each enzyme (ANOVA with a Tukey test or Welch's robust test with a Games-Howell test) at $P < 0.05$ level.

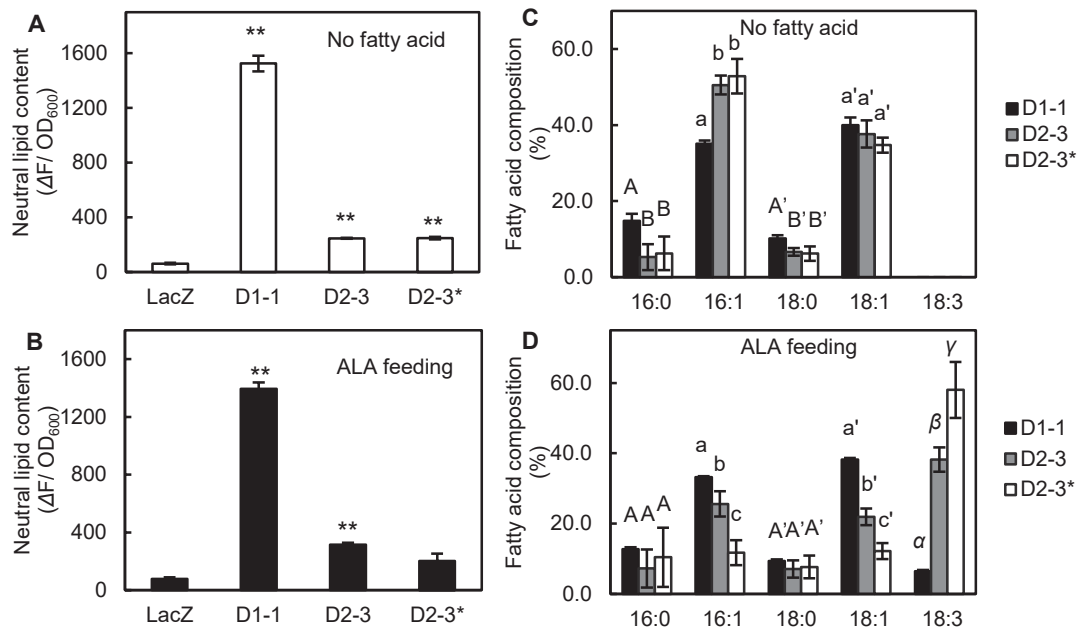


Figure 3. Effect of expressing flax *DGAT* in yeast H1246 on neutral lipid content and fatty acid composition of triacylglycerol. A and B, neutral lipid accumulation of yeast producing LuDGAT after 48 h induction. Neutral lipid content was measured by Nile red fluorescence. C and D, fatty acid composition (weight %) of triacylglycerol isolated from yeast producing LuDGAT. Yeast cells were cultured in the absence (A and C) or presence (B and D) of exogenous α -linolenic acid (ALA: 18:3) and harvested after 48 h induction. Data represent means \pm S.D. For A and B, $n = 2$ biological replicates. For C and D, $n = 3$ biological replicates. D1-1, LuDGAT1; D2-3, LuDGAT2-3; D2-3*, LuDGAT2-3 based on the codon-optimized cDNA. For A and B, the asterisks indicate significant differences in neutral lipid content of yeast expressing *LuDGAT* versus yeast expressing *LacZ* using t-test (** $P < 0.01$). For C and D, different letters in each series (non-primed uppercase letters for 16:0, non-primed lowercase letters for 16:1, primed uppercase letters for 18:0, primed lowercase letters for 18:1, and Greek letters for 18:3) indicate significant differences in the composition of each fatty acid from yeast producing different LuDGATs (ANOVA with a Tukey test or Welch's robust test with a Games-Howell test) at $P < 0.05$ level.

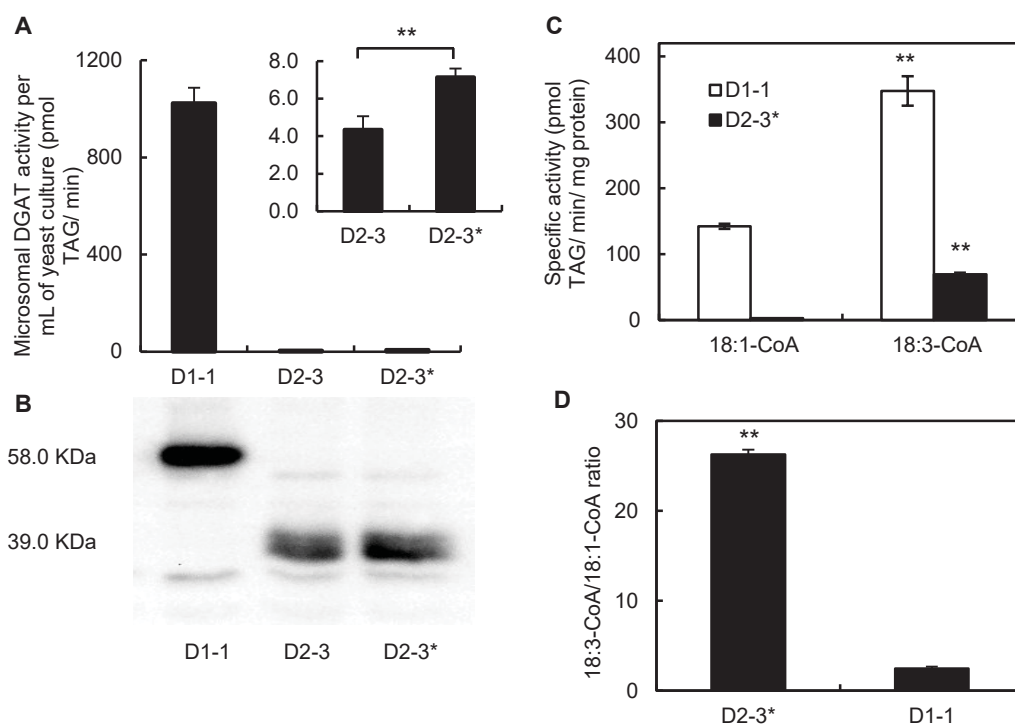


Figure 4. Enzyme activities and substrate specificities of LuDGATs. Microsomal preparations from the yeast mutant H1246 expressing *LuDGAT1* (D1-1), *LuDGAT2-3* (D2-3) or codon-optimized *LuDGAT2-3* (D2-3*) were used for analysis of enzyme assay and Western blotting. A, microsomal DGAT activities of recombinant D1-1, D2-3 and D2-3*. DGAT activity was assessed using 15 μ M [1- 14 C] oleoyl-CoA. B, protein accumulation of LuDGATs. The same batch of microsomes used to assess enzyme activity was used for Western blotting analysis. C, substrate specificity of LuDGAT towards oleoyl-CoA (18:1-CoA) or α -linolenoyl-CoA (18:3-CoA). D, ratio of substrate specificity towards 18:3-CoA versus 18:1-CoA of LuDGAT. Data represent means \pm S.D, n = 3. For A, C and D, the asterisks indicate significant differences (t-test) at P < 0.01 level.

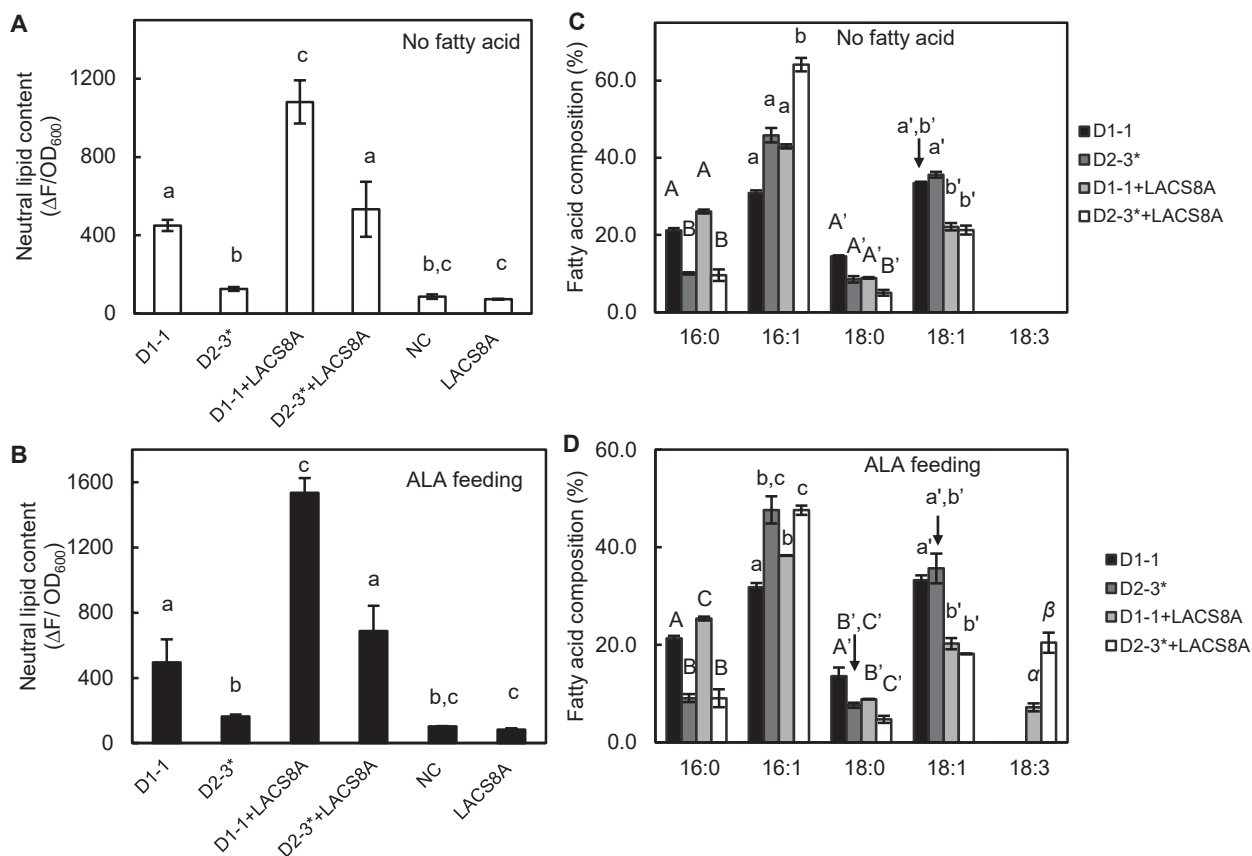


Figure 5. Effect of co-expressing *LuLACS8A* and *LuDGAT* in yeast mutant *BYQMfaal,4Δ* on neutral lipid content and fatty acid composition of triacylglycerol. A and B, neutral lipid accumulation of yeast co-expressing *LuLACS8A* and *LuDGAT* after 48 h induction. Neutral lipid content was measured by Nile red fluorescence. C and D, fatty acid composition (weight %) of triacylglycerol isolated from yeast co-expressing *LuLACS8A* and *LuDGAT*. Yeast cells were cultured in the absence (A and C) or presence (B and D) of exogenous α -linolenic acid (ALA) and harvested after 48 h induction. Data represent means \pm S.D, n = 3 biological replicates. D1-1, *LuDGAT1*; D2-3*, *LuDGAT2-3* encoded by codon-optimized cDNA. For A and B, different lowercase letters indicate significant differences in neutral lipid content (ANOVA with a Tukey test or Welch's robust test with a Games-Howell test) at $P < 0.05$ level. For C and D, different letters in each series (non-primed uppercase letters for 16:0, non-primed lowercase letters for 16:1, primed uppercase letters for 18:0, primed lowercase letters for 18:1, and Greek letters for 18:3) indicate significant differences in the composition of each fatty acid of TAG in the co-expression yeast (ANOVA with a Tukey test or Welch's robust test with a Games-Howell test) at $P < 0.05$ level.

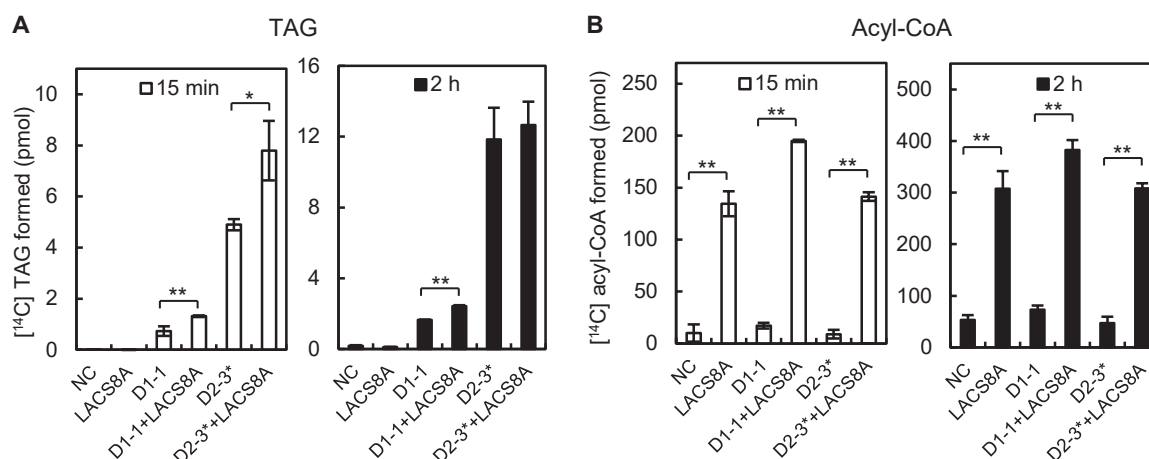


Figure 6. *In vitro* analysis of the cooperation between the reactions catalyzed by LuLACS8A and LuDGAT. Microsomal preparations from the yeast mutant *BYQMfaa1,4Δ* individually transformed with *pLACS8A+DGAT2-3**, *pDGAT2-3**, *pLACS8A+DGAT1-1*, *pDGAT1-1*, *pLACS8A* or *pNC* were incubated with [¹⁴C] α -linolenic acid, ATP, CoA and *sn*-1,2-diolein. After incubation, the reaction mixture was subjected to TLC and the amounts of the formed radiolabeled triacylglycerol (TAG) (A) and acyl-CoA (B) were calculated based on the radioactivity of the corresponding spots, respectively. Data represent means \pm S.D, n = 3. D1-1, LuDGAT1; D2-3*, LuDGAT2-3 encoded by codon-optimized cDNA. The asterisks indicate significant differences (t- test, *P < 0.05; **P < 0.01).

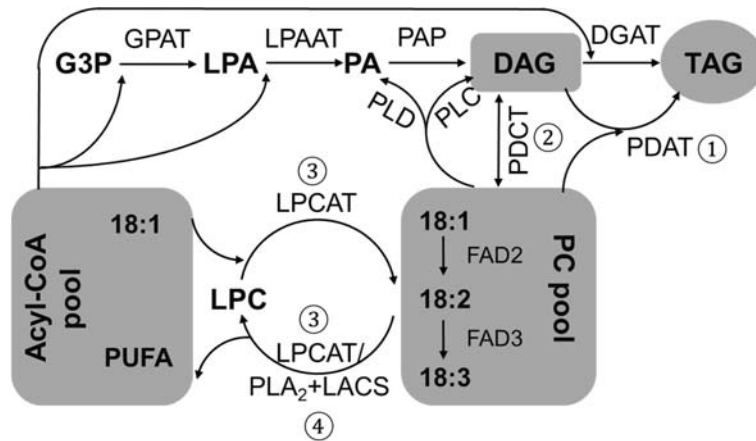


Figure 7. Four possible routes for enriching the α -linolenic acid (ALA; 18:3) content of triacylglycerol (TAG) during flax seed development. In route 1, phospholipid:diacylglycerol acyltransferase (PDAT) catalyzes the transfer of 18:3 from the *sn*-2 position of phosphatidylcholine (PC) enriched in 18:3 to *sn*-1,2-diacylglycerol (DAG) enriched in 18:3 to form 18:3-enriched TAG [1]. In route 2, phosphatidylcholine:diacylglycerol cholinephosphotransferase (PDCT) catalyzes the transfer of the phosphocholine headgroup of PC enriched in 18:3 to *de novo* DAG formed in the Kennedy pathway thus producing 18:3-enriched DAG for synthesis of TAG via either the PDAT or diacylglycerol acyltransferase (DGAT)-catalyzed reaction [6]. In route 3, coupling of the lysophosphatidylcholine acyltransferase (LPCAT)-catalyzed reverse reaction to the DGAT-catalyzed forward reaction results in the transfer of 18:3 from the *sn*-2 position of 18:3-enriched PC to the *sn*-3 position of DAG [30]. Use of 18:3-enriched DAG by route 3 would result in TAG highly enriched in 18:3. For route 4, the current study suggests that 18:3 can be channeled into TAG via the sequential actions of long chain acyl-CoA synthetase (LACS) and DGAT displaying enhanced specificity for substrate containing 18:3. Route 4 assumes that there is a phospholipase A₂ (PLA₂) which can selectively release free 18:3 from 18:3-enriched PC. Other abbreviations: FAD, fatty acid desaturase; GPAT, *sn*-glycerol-3-phosphate acyltransferase; G3P, *sn*-glycerol-3-phosphate; LPA, lysophosphatidic acid; LPAAT, lysophosphatidic acid acyltransferase; LPC, lysophosphatidylcholine; PA, phosphatidic acid; PAP, phosphatidic acid phosphatase; PLC, phospholipase C; PLD, phospholipase D; PUFA, polyunsaturated fatty acid.

1 **Appendix A. Supplementary material**

2 Supplementary Table S1. Sequences of the PCR primers employed in the current study.

3 *Restriction sites are indicated with underline and a Kozak translation initiation sequence is
4 indicated in italic.

5 Supplementary Table S2. Plasmids used in the current study.

6 Supplementary Table S3. Yeast strains used in the current study.

7 Supplementary Table S4. Predicted transmembrane domains (TMDs) in flax LACSs and AtLACSs
8 by TMpred, TMHMM, SOSUI or Phobius.

9 Supplementary Table S5. Overview of putative *LACS* cDNAs identified in flax.

10 Supplementary Table S6. Sequence identity and synonymous substitution rates (*Ks* values) of the
11 cDNA pairs.

12 Supplementary Figure S1. The predicted topology of LuLACS8A. The membrane topology of
13 LuLAC8A was predicted by Protter. Signature motifs and putative active sites based on the
14 structure of LACS from *Thermus thermophilus* are also indicated in the topology figure. The
15 putative active sites are represented by red-filled diamonds. The fatty acyl-CoA synthetase
16 signature motif (FACS signature motif) is represented by yellow-filled circles. The ATP/AMP
17 signature motifs are represented by blue-filled circles.

18 Supplementary Figure S2. LuLACSs complement yeast growth defect under oleic acid (OA)
19 auxotrophic conditions. The growth defect of yeast strain *BYfaal,4Δ* under fatty acid auxotrophic
20 conditions is rescued by LuLACSs. Serial dilutions of *BYfaal,4Δ* cells transformed with *LuLACS*
21 were spotted onto induction medium containing OA, or cerulenin, or both. Yeast mutant cells
22 containing AtLACS9 and control vector (*LacZ*) were used as positive and negative controls,
23 respectively.

24 Supplementary Figure S3. Expression of *LuLACS* in yeast mutant *BYfaal,4Δ* facilitates fatty acids
25 uptake in cell. A, neutral lipid accumulation of yeast mutant *BYfaal,4Δ* producing LuLACS. Data
26 represent means ± S.D, n = 4 biological replicates. B, amount of oleic acid (OA), linoleic acid (LA)
27 or α -linolenic acid (ALA) in triacylglycerol of yeast mutant *BYfaal,4Δ* producing LuLACS cultured
28 in medium supplemented with OA, LA or ALA, respectively. Yeast cells are harvested after 72 h
29 induction. Data represent means ± S.D, n = 2 biological replicates. The asterisks indicate significant

30 differences in neutral lipid content (A) of yeast expressing *LuLACS* versus yeast expressing *LacZ* (t-
31 test, *P < 0.05, **P < 0.01).

32

33

34 Table S1. Sequences of the PCR primers employed in the current study. *Restriction sites are
 35 indicated with underline and a Kozak translation initiation sequence is indicated in italic.

Primer name	Sequence*
Primers used for pYES2.1 cloning of <i>LuLACS</i> cDNAs	
AtLACS9-F	5'-GCAGAGCGGCCGCATGATTCCTTATGCTGCTGGTG-3'
AtLACS9-R	5'-TATGTCGACGGCATATAACTTGGTGAGATCTTCA-3'
LuLACS8A-F	5'-GCAGAGCGGCCGC <i>ACA</i> ATGGCAGATCCGGAGGGG-3'
LuLACS8A-R	5'-TATGTCGACATGATAGAGCTTCTGCAGTTCATCTT-3'
LuLACS9A-F	5'-GCAGAGCGGCCGCATGAGCGTGTACGTGATCG-3'
LuLACS9A-R	5'-TATGTCGACTTCATATAGCTCAGCTAGCTCTTCAG-3'
LuLACS9C-F	5'-GCAGAGCGGCCGCATGACCCTGTACCTGATCAT-3'
LuLACS9C-R	5'-TATGTCGACAGATTCATACATCTTAGATAGATCTTCAG-3'
Primers used for pYES-NTA or pESC cloning of <i>LuDGATs</i>	
LuDGAT1-1-F	5'-TATAGGATCC <i>ACACA</i> ATGTCCGTGCTAGACACTCCT-3'
LuDGAT1-1-R	5'-TATACTCGAGTTAGATTCATCTTTCCATTCC-3'
LuDGAT2-3-F	5'-TATAGGATCC <i>ACACA</i> ATGTCCGTACAGAAAGTAGAGGAGG-3'
LuDGAT2-3-R	5'-TATACTCGAGTTAAAGAATTTTGAGTTGAAGATCAGC-3'
Codon optimized-LuDGAT2-3-F	5'-TATAGGATCC <i>ACACA</i> ATGTCCGTTACAGAAAGTCGAA-3'
Codon optimized-LuDGAT2-3-R	5'-TATACTCGAGTTACAAGATTTTCAACTGAAGATCCG-3'
Primers used for cloning co-expression constructs	
pESC-F	5'-GAGAGGCGTTTTGCGTATTGGGCGCGCTGAATTGGAGCGACCTCATGC-3'
pESC-R	5'-GTCAGTGAGCGAGGAAGCGGAAGACTGGATCTTCGAGCGTCCCAAAACC-3'
pYES-F	5'-GGTTTTGGGACGCTCGAAGATCCAGTCTTCCGCTTCTCGCTCACTGAC-3'
pYES-R	5'-GCATGAGGTGCGTCCAATTCAGCGCGCCAATACGCAAACCGCCTCTC-3'

36

37 Table S2. Plasmids used in the current study.

Plasmid name	Description
pYES-LACS8A	pYES- P _{GALI} - LACS8A-V5 tag-T _{CYC1}
pYES-LACS9A	pYES- P _{GALI} - LACS9A-V5 tag-T _{CYC1}
pYES-LACS9C	pYES- P _{GALI} - LACS9C-V5 tag-T _{CYC1}
pYES-DGAT1-1	pYES- P _{GALI} - His tag-DGAT1-1-T _{CYC1}
pYES-DGAT2-3	pYES- P _{GALI} - His tag-DGAT2-3-T _{CYC1}
pYES-DGAT2-3*	pYES- P _{GALI} - His tag-codon optimized DGAT2-3-T _{CYC1}
pLACS8A+DGAT1-1	pYES-P _{GALI} -LACS8A-T _{CYC1} /P _{GALI} - DGAT1-1-T _{CYC1}
pLACS8A+DGAT2-3*	pYES-P _{GALI} -LACS8A-T _{CYC1} /P _{GALI} -codon optimized DGAT2-3-T _{CYC1}
pLACS8A	pYES-P _{GALI} -LACS8A-T _{CYC1} /P _{GALI} -T _{CYC1}
pDGAT1-1	pYES-P _{GALI} -T _{CYC1} /P _{GALI} - DGAT1-1-T _{CYC1}
pDGAT2-3*	pYES-P _{GALI} -T _{CYC1} /P _{GALI} -codon optimized DGAT2-3-T _{CYC1}
pNC	pYES-P _{GALI} - T _{CYC1} /P _{GALI} -T _{CYC1}

38

39

40 Table S3. Yeast strains used in the current study.

Strain name	Genotype
Wild type <i>S. cerevisiae</i> strain BY4742	<i>MATα, his3Δ1, leu2Δ0, lys2Δ0, ura3Δ0</i>
<i>BYQMfaa1,4Δ</i>	<i>MATα, his3Δ1, leu2Δ0, lys2Δ0, ura3Δ0, dga1 Δ::kanMX, lro1 Δ::kanMX, are1 Δ::kanMX, are2 Δ::kanMX, faa1 Δ::HIS3, faa4 Δ::LYS2</i>
<i>BYfaa1,4Δ</i>	<i>MATα, his3Δ1, leu2Δ0, lys2Δ0 ura3Δ0, faa1 Δ::HIS3, faa4 Δ::LYS2</i>
<i>S. cerevisiae</i> strain H1246	<i>MATα are1-Δ::HIS3, are2-Δ::LEU2, dga1-Δ::KanMX4, lro1-Δ::TRP1 ADE2</i>

41

42

43

44

45

46

47

48 Table S4. Predicted transmembrane domains (TMDs) in flax LACSs and AtLACSs by TMpred,
 49 TMHMM, SOSUI or Phobius.

	TMpred	TMHMM	SOSUI	Phobius
AtLACS8	18-41 179-197 274-294 335-353	20-42 167-189	19-41	20-41
No. of TMD	4	2	1	1
AtLACS9	1-18 262-285 307-327 584-604		1-20	
No. of TMD	4	0	1	0
LuLACS8A	35-57 303-326 347-365	35-57	34-56	32-55
No. of TMD	3	1	1	1
LuLACS9A	1-18 106-124 243-264 267-286 388-409		1-18	
No. of TMD	5	0	1	0
LuLACS9C	1-21 265-289 310-330 386-407	2-21	2-23	6-23
No. of TMD	4	1	1	1

50

51 Table S5. Overview of putative *LACS* cDNAs identified in flax.

Genes	cDNA length (bp)	Protein length (Amino acid)	Molecular mass (KDa)	Isoelectric point
<i>LuLACS8A</i>	2199	732	79.667	6.19
<i>LuLACS8B</i>	2193	730	79.499	5.94
<i>LuLACS9A</i>	2091	696	76.227	7.52
<i>LuLACS9B</i>	2091	696	76.052	6.85
<i>LuLACS9C</i>	2088	695	75.646	8.59
<i>LuLACS9D</i>	2088	695	75.455	8.50

52

53 Table S6. Sequence identity and synonymous substitution rates (*Ks* values) of the cDNA pairs.

cDNA Pair	Nucleotide (%)	Amino Acid (%)	<i>Ks</i> (mean±S.E.)	<i>Ks</i> average
<i>LuLACS8A</i> and <i>LuLACS8B</i>	96.2	96.6	0.09951 ± 0.01370	0.083
<i>LuLACS9A</i> and <i>LuLACS9B</i>	97.2	98.3	0.09170 ± 0.01373	
<i>LuLACS9C</i> and <i>LuLACS9D</i>	97.7	98.1	0.05791 ± 0.01021	

54

55

56

57

58

59

60

61

62

63

64

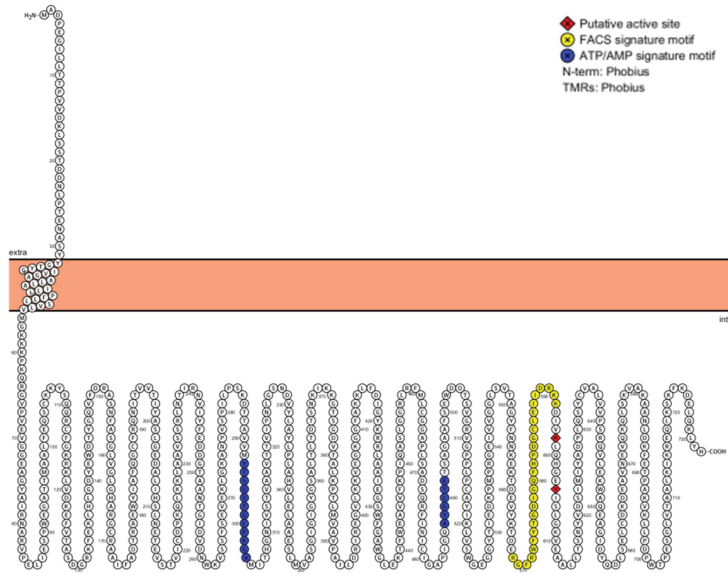
65

66

67

68

69



70

Figure S1. The predicted topology of LuLACS8A. The membrane topology of LuLACS8A was

71

predicted by Protter. Signature motifs and putative active sites based on the structure of LACS from

72

Thermus thermophilus are also indicated in the topology figure. The putative active sites are

73

represented by red-filled diamonds. The fatty acyl-CoA synthetase signature motif (FACS signature

74

motif) is represented by yellow-filled circles. The ATP/AMP signature motifs are represented by

75

blue-filled circles.

76

77

78

79

80

81

82

83

84

85

86

87

88

89

90

91

92

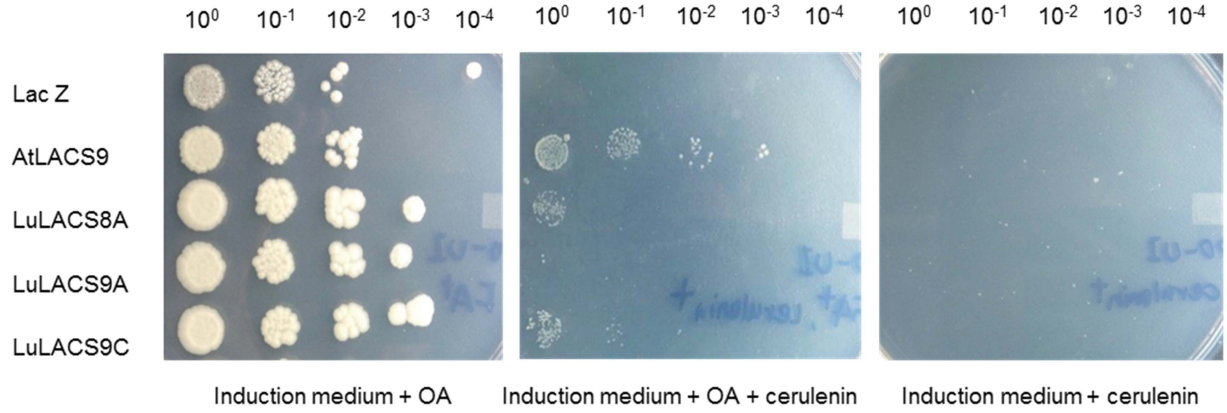


Figure S2. LuLACSs complement yeast growth defect under oleic acid (OA) auxotrophic conditions. The growth defect of yeast strain *BYfaa1,4Δ* under fatty acid auxotrophic conditions is rescued by LuLACSs. Serial dilutions of *BYfaa1,4Δ* cells transformed with *LuLACS* were spotted onto induction medium containing OA, or cerulenin, or both. Yeast mutant cells containing AtLACS9 and control vector (LacZ) were used as positive and negative controls, respectively.

93

94

95

96

97

98

99

100

101

102

103

104

105

106

107

108

109

110

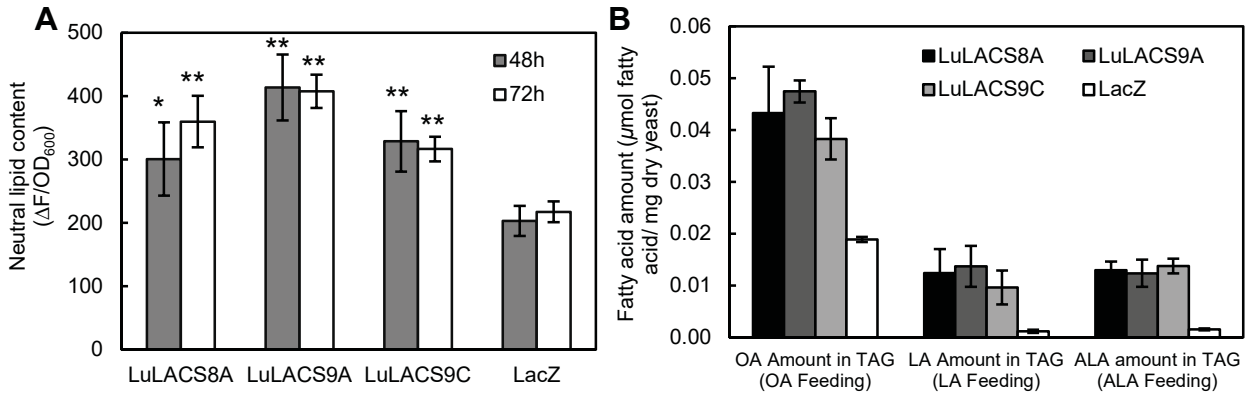


Figure S3. Expression of *LuLACS* in yeast mutant *BYfaal,4Δ* facilitates fatty acids uptake in cell. A, neutral lipid accumulation of yeast mutant *BYfaal,4Δ* producing *LuLACS*. Data represent means \pm S.D, n = 4 biological replicates. B, amount of oleic acid (OA), linoleic acid (LA) or α -linolenic acid (ALA) in triacylglycerol of yeast mutant *BYfaal,4Δ* producing *LuLACS* cultured in medium supplemented with OA, LA or ALA, respectively. Yeast cells are harvested after 72 h induction. Data represent means \pm S.D, n = 2 biological replicates. The asterisks indicate significant differences in neutral lipid content (A) of yeast expressing *LuLACS* versus yeast expressing *LacZ* (t-test, *P < 0.05, **P < 0.01).